AD-A191 721 MICROWAVE LANDING SYSTEM MATHEMATICAL MODELING STUDY FOR MIDWAY AIRPORT R..(U) FEDERAL AVIATION ADMINISTRATION TECHNICAL CENTER ATLANTIC CIT.. 1/1

UNCLASSIFIED J D JONES ET AL. JAN 88 DOT/FAA/CT-TN87/49 F/G 17/7.3 NL

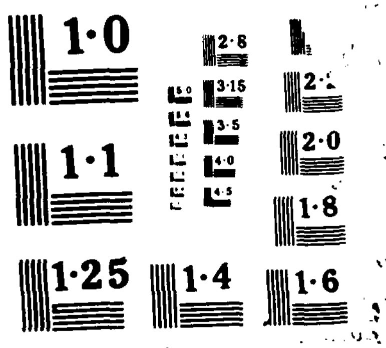
1·0
2·8
3·15
3·5
4·0
4·5
5·0
2·0
1·1
1·8
1·25
1·4
1·6

technical note technical note tech

(2)

AD-A191 721

Microwave Landing System Mathematical Modeling Study for Midway Airport Runway 22L, Chicago, Illinois

Jesse D. Jones
Linda Epstein

DISTRIBUTION STATEMENT A
Approved for public release;
Distribution Unlimited

January 1988

DOT/FAA/CT-TN87/49

This document is available to the U.S. public through the National Technical Information Service, Springfield, Virginia 22161.

US Department of Transportation
Federal Aviation Administration

Technical Center
Atlantic City International Airport, N.J. 08405

Technical Report Documentation Page

1. Report No. DOT/FAA/CT-TN87/49	2. Government Accession No.	3. Recipient's Catalog No.
4. Title and Subtitle MICROWAVE LANDING SYSTEM MATHEMATICAL MODELING STUDY FOR RUNWAY 22L, MIDWAY AIRPORT, CHICAGO, ILLINOIS		5. Report Date January 1988
		6. Performing Organization Code ACT-140
7. Author(s) Jesse D. Jones and Linda Epstein		8. Performing Organization Report No. DOT/FAA/CT-TN87/49
9. Performing Organization Name and Address U.S. Department of Transportation Federal Aviation Administration Technical Center Atlantic City International Airport, N.J. 08405		10. Work Unit No. (TRAIS)
		11. Contract or Grant No. T0603N
12. Sponsoring Agency Name and Address U.S. Department of Transportation Federal Aviation Administration Program Engineering and Maintenance Service Washington, D.C. 20590		13. Type of Report and Period Covered Technical Note August through October 1987
		14. Sponsoring Agency Code

15. Supplementary Notes

16. Abstract

This technical note describes microwave landing system (MLS) mathematical modeling performed for runway 22L, Midway Airport, Chicago, Illinois. This study considered multipath and shadowing effects of buildings and aircraft. Results are provided as plots showing the multipath levels and separation angles and error plots showing the resultant errors.

17. Key Words Midway Airport MLS Microwave Landing System Mathematical Modeling	18. Distribution Statement This document is available to the U.S. public through the National Technical Information Service, Springfield, Va. 22161

19. Security Classif. (of this report)	20. Security Classif. (of this page)	21. No. of Pages	22. Price
Unclassified	Unclassified	66	

Form DOT F 1700.7 (8-72) Reproduction of completed page authorized

TABLE OF CONTENTS

LIST OF TABLES

LIST OF ILLUSTRATIONS

LIST OF ILLUSTRATIONS (CONTINUED)

EXECUTIVE SUMMARY

A microwave landing system (MLS) mathematical modeling study was performed for Runway 22L, Midway Airport, Chicago, Illinois. A brief model description is included in the report explaining its organization and capabilites. This study considered the static effects of fixed objects and the transient effects of aircraft likely to be found at Midway.

Ten buildings and 10 aircraft were modeled for multipath effects. Six buildings and one aircraft were modeled for shadowing effects. Results indicate that MLS performance would be within error tolerances. However, plots of the orbital flightpath indicate the possibility of an out-of-tolerance condition between -24° and -26° due to the shadowing effects of buildings 7 and 8 (new Beckett Aviation hangar). These effects will be negligible if the approach procedure keeps the aircraft at 3000 feet mean sea level (m.s.l.) or higher in the vicinity of these radials.

INTRODUCTION

OBJECTIVE.

To identify the magnitude of the potential derogatory effects of the Midway Airport environment at Chicago, Illinois, upon a microwave landing system (MLS) precision approach to runway 22L.

BACKGROUND.

Precision MLS approach guidance path performance may be derogated by the effects of reflections (multipath) from buildings, aircraft, and ground, as well as the diffraction and blockage effects (shadowing) of buildings and aircraft. A computer program (mathematical model) has been developed to simulate these effects based upon user inputs describing the applicable airport scenario. This program is described by the reports listed in the bibliography. Appendix A provides a summary description of the math model.

Although Congress has mandated an instrument landing system (ILS) installation for Midway Airport runway 22L in the FY-87 supplemental budget, the Great Lakes region has determined that an ILS installation is impractical to site. This determination was based upon a hostile multipath environment and a required 3.6° glidepath for obstacle clearance of the downtown Sears building. Subsequently, since Midway 22L already exists as part of the Hazeltine MLS contract, it has been moved up in priority to provide an MLS approach by November 1988. This mathematical modeling study was performed to determine if there are any significant multipath effects which would prevent the commissioning of a runway 22L MLS installation.

MLS MODEL INPUT CONSIDERATIONS

This simulation was based upon a "quick-look" philosophy in that several short-cuts were applied in determining input data. The sites selected were based on nominal locations with only a cursory consideration of all siting regulations involved. The coordinates used for buildings and aircraft were from the digitizing tablet supported by nominal field survey measurements and will differ from values obtained by a rigorous site survey. Building heights were calculated from the field survey measurements, although the reference locations were not surveyed exactly. However, this is not expected to have any noticeable impact on the output.

1. Coordinate Systems. The MLS mathematical model uses the runway centerline as the X-axis with the "0" value of the X and Y axes corresponding to the stop end of the runway. The Z-axis "0" reference is chosen as the lowest mean sea level (m.s.l.) value along the runway which is the threshold (displaced) of runway 22L at Midway. MLS coverage requirements and error plots are based on a coordinate system centered on the MLS datum point (point on runway centerline opposite the Elevation (EL) subsystem).

2. Approach Paths. The approach path descent is simulated beginning at 6.242 nautical miles (nmi) from threshold (3000 feet. m.s.l.), continuing along

the 3.6° glide slope to a point 8 feet above the runway surface and then over the runway to the stop end remaining at 8 feet above the runway surface. In addition, the lower coverage limit is checked with a 10 nmi orbit at 0.9° elevation angle referenced to the MLS datum point from -40° to +40° horizontally referenced to the MLS datum point and the runway centerline.

3. Multipath Effects. A total of 11 buildings was simulated for multipath. The 10 existing and proposed buildings with the highest multipath levels were included in the final model runs. The buildings modeled with corresponding reference numbers (used in figure 1 and tables 2, 5, and 6) are as follows:

Bldg. No.	Description Based on Future Airport Layout Plan
1	Monarch hangar
2	Monarch hangar
3	Proposed corporate hangar
4	Esmark hangar installation
5	Monarch and Butler hangars
6	Midway Airlines hangar
7	Beckett new hangar office area
8	Beckett new hangar
9	ATC tower north side
10	ATC tower west side

A total of 15 aircraft (B-727's) were also simulated at various locations on the airport taxiways and ramp areas. This number was reduced to the 10 most likely to cause problems based upon multipath levels. Aircraft locations simulated on the ramp areas were based upon aerial photographs. The modeled aircraft with corresponding reference numbers (used in figure 1 and tables 2, 5, and 6) are as follows:

A/C No.	Description Based on Future Airport Layout Plan
3	On north ramp between runways 22R and 22L
4	Holding on taxiway east of runway 4R stop end
5	Holding on taxiway near existing displaced runway 22L threshold
6	Parked north of concourse C
7	Parked south of concourse C
8	Parked north of concourse B near tower
9	On runway 4R/22L taxiway just south of runway 13R/31L taxiway
10	On runway 13R just north of runway 4R/22L
12	Parked at northwest corner of concourse B
15	On 4R/22L taxiway just north of south taxiway

Although the downtown Sears building and other nearby skyscrapers are an obstruction problem, they were not considered in this modeling study since the approach path modeled did not extend beyond downtown Chicago. The approach path modeled was the only specific path available since an approach procedure for a Midway 22L MLS approach has not been developed yet. When the approach procedure is determined, additional modeling should be performed for that approach path.

4. Shadowing Effects. Shadowing effects include both blockage by an object and diffraction around the object. The effects of a shadowing aircraft on the azimuth subsystem were simulated by an aircraft taking off from runway 13R. To simulate a worst case condition, the interfering aircraft just crossed runway 22L when the aircraft making an MLS approach to runway 22L was over the threshold. The effects of six shadowing buildings were also simulated. The buildings included were identified above as numbers 5, 6, 7, 8, 9, and 10.

DATA PRESENTATION AND ANALYSIS

Input data unique to this scenario are listed in table 1, MLS Input Parameters, and table 2, Scenario Obstacle Data. These tables list the transmitter locations, building locations, etc., used for this simulation. A detailed explanation of the various input parameters is provided in appendix B. An airport scenario map showing the relationship of the runway and transmitters to the multipath sources and shadowing objects is shown in figure 1. Building locations are represented by rectangles (wide lines) and are referenced to table 2 by the adjacent numbers. Aircraft locations are indicated by arrow shaped symbols and may be referenced to table 2 by the number following the "A." The tip of the arrow indicates the aircraft nose. Waypoint and segment parameters used for the centerline approach are listed in table 3. Currently, the orbital flightpath can only be simulated by a series of segments. The waypoint and segment parameters for the orbital flightpath are provided in table 4. The orbital flightpath was simulated at 10 nmi, as opposed to the 20 nmi coverage limit, in order to minimize computer run time and the number of data points. The altitude used for the orbital flightpath places the aircraft at the lower coverage limit.

The maximum values for multipath from the ground, buildings, and aircraft are ranked and listed in table 5 for the centerline approach and in table 6 for the orbital flightpath. Diagnostic plots show the "Multipath/Direct" (M/D) ratio for all Azimuth (AZ), EL, Precision Distance Measuring Equipment (DME/P)) subsystems. In addition, "Separation Angle" plots are provided for the angle equipment, and "Relative Time Delay" plots are provided for the DME/P. In the upper right corner of the diagnostic plots is a legend indicating which multipath sources correspond with the plot symbols. The legend list is for the highest six multipath sources and is ranked accordingly. The solid line on the M/D plots is used to connect the data points for the highest ranked multipath source. Values are plotted on the separation angle plots only when the corresponding Multipath/Direct (M/D) ratio is above -40 decibels (dB). The solid line on the separation angle plots is used to connect the symbols where the multipath exists continuously over several samples.

Figures 2 and 3 are the M/D and separation angle plots, respectively, for the AZ subsystem. These plots have an expanded X-axis to show the multipath effects near threshold more clearly since no multipath effects occur on the approach beyond 1 nmi from threshold. The six highest multipath sources (ranked 1 through

6 in table 5 for AZ) are shown on these plots as identified by the legend in the upper right corner. Although building 6 shows a multipath level within 1 dB of the direct signal in the touchdown zone, the separation angle exceeds 10° in this area. The multipath from buildings 7 and 8 occurs further down the runway, and again the multipath is associated with large separation angles. Similarly, for the remaining buildings and aircraft, the separation angle for the multipath sources is large enough (greater than 2 beam widths) and the M/D ratio is low enough to prevent any significant problems. Therefore, no significant AZ errors are expected due to multipath from aircraft or buildings.

The M/D and time delay diagnostic plots for the DME/P subsystem are provided in figures 4 and 5, respectively. These plots also have an expanded X-axis to show the multipath effects near threshold more clearly since no multipath effects occur on the approach beyond 1 nmi from threshold. The six highest multipath sources (ranked 1 through 6 in table 5 for DME/P) are shown on these plots, as identified by the legend in the upper right corner. Building 6 is shown to have a multipath level approaching that of the direct signal. However, the associated time delay is in excess of 700 nanoseconds (ns) which should eliminate any errors. The multipath from building 8 is shown to come within 2 dB of the direct signal in an area where the time delay is about 300 ns. This could cause some accuracy errors. However, this would occur approximately 3000 feet past threshold and, therefore, should not be a concern. For the remaining buildings and aircraft no accuracy errors are expected due to low multipath levels (more than 3 dB below the direct) or long time delays (greater than 350 ns).

Diagnostic plots for the EL subsystem are shown by figures 6 and 7. These plots also have an expanded X-axis to show the multipath effects near threshold more clearly since no multipath effects occur on the approach beyond 1 nmi from threshold. The six highest multipath sources (ranked 1 through 6 in table 5 for EL) are shown on these plots, as identified by the legend in the upper right corner. These plots must be examined with caution to avoid any misconceptions. High multipath levels are seen behind the EL antenna and should be ignored because the model is omnidirectional at this stage. Antenna directivity is considered subsequently in the system part of the model. The highest level of multipath to consider is the in-beam multipath from aircraft 6. However, the low M/D ratio (below -19 dB) should preclude any errors.

Shadowing effects to the AZ subsystem are shown in figure 8. The amplitude fluctuations are caused by ground lobing effects since the shadowing simulation includes ground reflection computations. The above comments also apply to the DME/P shadowing plot in figure 9. No shadowing effects are shown on the EL plot in figure 10 since the aircraft are behind the EL subsystem and the beam is shaped to minimize ground reflections.

The Time Reference Scanning Beam (TRSB) receiver simulation routine processes the multipath generated in the propagation part of the model to determine AZ and EL angle errors. This processing is modeled after an actual receiver flow chart and includes such features as dwell gate or split gate processing (dwell gate used for this simulation), acquisition, tracking, system flags, coast mode, and slew rate limiting. The transmitter radiation patterns (Hazeltine 2° AZ and 1.5° EL) and aircraft antenna patterns are also applied at this point in the processing. The raw error from the simulation is further processed by passing it through Path Following Error (PFE) and Control Motion Noise (CMN) filters. The equations used to implement the filters are based on the application of a Bilinear

Transformation to the transfer function (see appendix C). Other than the addition of the 10 radians per second low-pass filter to the CMN calculation, the equations are equivalent to those being used for other MLS data processing activities. Simulation of a DME/P interrogator is not currently included in the model program.

Figures 11, 12, and 13 are the Raw error, PFE filtered, and CMN filtered plots, respectively, for the AZ subsystem. Although considerable raw errors are observed in figure 11, the filtered errors are well within the tolerance limits as shown in figures 12 and 13. The EL subsystem Raw error, PFE, and CMN plots are provided in figures 14, 15, and 16. The spike near the end of the valid elevation information is attributed to conical angle effects. Due to the lack of significant multipath effects, no out-of-tolerance errors are evident. However, the errors shown are attributed to the air traffic control (ATC) tower and building 4 (scheduled for demolition).

To check for potential problems in the coverage area away from centerline, an orbit was simulated at the lower coverage limit (0.9° 964 feet above ground). This type of simulation also provides the diagnostic, raw, and filtered error plots. Figures 17 and 18 show the orbital M/D and separation angle plots for the AZ subsystem. The azimuth radials which would be subjected to multipath can be readily identified in figure 17 as -42°, -27° through -20°, and +3°. The highest multipath observed occurs at -24.8° from building 8 (see table 6 for AZ) and exceeds the level of the direct signal (3.23 dB). Building 7, which is part of building 8, also provides a multipath level in excess of the direct signal (1.73 dB). The separation angles for these buildings are much greater than 2 beam widths, and no out-of tolerance errors are expected. The multipath levels from the other buildings are low enough and the separation angles large enough to preclude any significant errors. Orbital M/D and time delay plots for the DME/P are provided by figures 19 and 20. Radials where multipath could affect the DME/P are easily seen in figure 19 to be the same as the AZ. These multipath levels are all more than 3 dB below the direct signal which should preclude any significant accuracy effects. However, due to the short time delays near -41° from buildings 1, 2, and 3 (less than 350 ns), this issue should be addressed by the contractor. Building 4 is scheduled for demolition; therefore, the effects near +4° may be disregarded. EL subsystem plots for M/D and separation angle from the orbital flightpath are shown in figures 21 and 22. Potential problems exist from the ATC tower (building 9) due to the high level of in-beam multipath near +12.7°. However, since the tower is located about 82° from the EL boresight, the amount of signal available at this angle due to the application of the antenna patterns is minimal, and any resulting errors are expected to be within tolerances.

Shadowing plots for the orbital flightpath begin with figure 23 for the AZ subsystem. The constant 5 dB bias in this plot is attributed to the ground lobing associated with the shadowing simulations. The amplitude change between -31° to -25° is attributed to the diffraction effects of building 5. The shadowing effects of building 6 are seen between -15° to -12°. The ATC tower effects on the AZ signal can be observed at about +12°. The effects of buildings 7 and 8 are between 22° through 32°. DME/P shadowing effects are presented by figure 24. Due to the difference in frequencies, the bias and magnitude of shadowing effects are different. However, the buildings causing AZ shadowing effects also affect the DME/P at the same angles due to collocation of the sites. The only shadowing effect apparent to the EL subsystem is the constant bias due to ground lobing (see figure 25).

Raw error, PFE filtered, and CMN filtered plots are provided for the AZ subsystem in figures 26, 27, and 28. The errors generated near -25° are attributed to the multipath effects of building 8, whereas, the effects near +25° are caused by the diffraction effects (shadowing) of building 8. The shadowingeffects of the ATC tower are observed near +12°. The shadowing effects of building 8 cause an out-of-tolerance condition between 22° and 30° as shown by figures 27 and 28. Otherwise, all errors are within tolerances. Orbits simulated at higher altitudes of 2000 and 3000 feet above ground showed considerably less shadowing effects and resulted in AZ errors which were within tolerance (the plots are not included). The Raw error, PFE, and CMN plots generated by the orbital flightpath for the EL subsystem are shown in figures 29, 30, and 31, respectively. Errors from building 4 (which is scheduled for demolition) near centerline are evident on the EL subsystem plots. However, all errors fall well within the dashed error tolerance lines of figures 30 and 31.

SUMMARY

The approach in modeling this airport was to identify potential problem areas prior to the MLS equipment installation. Subsystem locations modeled are based upon nominal siting considerations and are expected to conform with the latest siting criteria. Building coordinates (X and Y) were obtained from a [illegible] tablet with additional data obtained from a cursory site survey. Due to map scale, parallax, and tablet resolution, these values will differ from those obtained by a rigorous field survey. Building heights were either estimated [illegible] obstruction chart data or computed from field survey data. Due to assump[illegible] made in the model, the results presented here are considered "worst-case" whereas, the actual effects of multipath and shadowing are expected [illegible] than shown. However, any areas of the approach and the orbit ind[illegible] potential problems should be addressed by the contractor in the [illegible] report.

In this scenario, the buildings (modeled as smooth, perfect refle[illegible] aircraft create mainly out-of-beam and low levels of multipath. There[illegible] location is expected to be free of any significant multipath pro[illegible] approach. The results of the orbit indicate that the AZ and DME/P [illegible] performance could be affected by diffraction (shadowing) from buildings [illegible] (new Beckett Aviation hangar). An out-of-tolerance condition results [illegible] lower coverage limit between -24° through -26°. If the approach pr[illegible] keeps the aircraft at 3000 feet above ground or higher in the vicinity [illegible] radials, however, the shadowing effects of these buildings will be neg[illegible] We recommend further modeling of the approach procedures when they are fi[illegible]

BIBLIOGRAPHY

1. MLS Multipath Studies Volume I: Mathematical Models and Validation, Massachusetts Institute of Technology, Lincoln Laboratory, Lexington, Massachusetts, report number FAA-RD-76-3,1 (ATC-63 Volume I), February 25, 1976.

2. MLS Multipath Studies Volume II: Mathematical Models and Validation, Massachusetts Institute of Technology, Lincoln Laboratory, Lexington, Massachusetts, report number FAA-RD-76-2,1 (ATC Volume II), February 25, 1976.

3. Multipath Parameter Computations for the MLS Simulation Computer Program, Massachusetts Institute of Technology, Lincoln Laboratory, Lexington, Massachusetts, report number FAA-RD-76-55 (ATC-68), April 8, 1976.

TABLE 1. MIDWAY RUNWAY 22L, MLS INPUT PARAMETERS

PROGRAM TO DO MULTIPATH MODELING AND SIMULATION OF MLS - INPUT PARAMETERS

RUN IDENTIFICATION : 0816
RUN TITLE : MIDWAY 3.6 DEGREE APPROACH
AIRPORT : MIDWAY AIRPORT, CHICAGO, ILLINOIS
RUNWAY : 22L
RUNWAY LENGTH : 5346. FEET
RUNWAY WIDTH : 150. FEET
APPROACH REFERENCE DATUM HEIGHT : 55. FEET
MINIMUM GLIDE PATH ANGLE : 4. DEG

PARAMETERS FOR AZIMUTH SYSTEM:

PARAMETER	VALUE	UNITS
AZIMUTH X	-350.00	FEET
AZIMUTH Y	0.00	FEET
AZIMUTH Z	17.00	FEET
AZ FREQUENCY	5000.00	MHZ

PARAMETERS FOR DME/P SYSTEM:

PARAMETER	VALUE	UNITS
DME/P X	-350.00	FEET
DME/P Y	6.00	FEET
DME/P Z	30.75	FEET
DME/P FREQUENCY	1000.00	MHZ

PARAMETERS FOR ELEVATION SYSTEM:

PARAMETER	VALUE	UNITS
ELEVATION X	4614.70	FEET
ELEVATION Y	325.00	FEET
ELEVATION Z	8.99	FEET
EL FREQUENCY	5000.00	MHZ

MULTIPATH EDITING PARAMETERS

THRESHOLDS FOR EACH PASS:
PASS 1 = 0.10E-04
PASS 2 = 0.10E-01
PASS 3 = 0.30E-01

OUT OF BEAMNESS:

AZIMUTH = 3.00 DEG
DME/P = 0.50E-05 SEC
ELEVATION = 3.00 DEG

TABLE 2. MIDWAY RUNWAY 22L, SCENARIO OBSTACLE DATA

PARAMETERS USED IN COMPUTATION OF MULTIPATH REFLECTIONS *************************

BUILDING PARAMETERS ARE:

ID	XL	YL	XR	YR	HB	HBOT	SH2B	ERBR	ERBI	TILT
1	861.	1425.	989.	1556.	50.	5.	0.0000	0.10E+01	-0.10E+09	0.000
2	1077.	1642.	1232.	1800.	54.	5.	0.0000	0.10E+01	-0.10E+09	0.000
3	1774.	2356.	1875.	2456.	33.	5.	0.0000	0.10E+01	-0.10E+09	0.000
4	6070.	370.	6470.	370.	60.	0.	0.0000	0.10E+01	-0.10E+09	0.000
5	4003.	2610.	4392.	2209.	50.	0.	0.0000	0.10E+01	-0.10E+09	0.000
6	4990.	1676.	5404.	1256.	43.	0.	0.0000	0.10E+01	-0.10E+09	0.000
7	1430.	-760.	1500.	-760.	28.	10.	0.0000	0.10E+01	-0.10E+09	0.000
8	1150.	-750.	1430.	-750.	47.	10.	0.0000	0.10E+01	-0.10E+09	0.000
9	4830.	-1028.	4804.	-1000.	76.	15.	0.0000	0.10E+01	-0.10E+09	0.000
10	4800.	-999.	4778.	-1026.	76.	15.	0.0000	0.10E+01	-0.10E+09	0.000

ERG= 3.0000 -0.9000 SH2G= 0.605

AIRCRAFT PARAMETERS ARE:

ID	XT	YT	XC	YC	NACTYP	ALT	GRNDAC
3	5528.0	694.0	5612.0	606.0	3	10.0	0.0
4	6050.0	-259.0	6050.0	-135.0	3	10.0	0.0
5	5500.0	-270.0	5500.0	-152.0	3	11.0	0.0
6	5189.0	-352.0	5104.0	-435.0	3	11.0	0.0
7	4874.0	-564.0	4959.0	-484.0	3	11.0	0.0
8	4692.0	-686.0	4610.0	-769.0	3	11.0	0.0
9	1976.0	-400.0	2097.0	-400.0	3	14.0	2.0
10	2420.0	254.0	2420.0	134.0	3	14.0	2.0
12	4407.0	-405.0	4327.0	-490.0	3	11.0	0.0
15	622.0	-400.0	748.0	-400.0	3	24.0	7.0

PARAMETERS USED IN COMPUTATION OF SHADOWING **************************************

BUILDING PARAMETERS ARE:

ID	SHBLD: XL	YL	XR	YR	HBS	HBT
5	4003.0	2610.0	4392.0	2209.0	50.0	0.0
6	4990.0	1676.0	5404.0	1256.0	43.0	0.0
7	1430.0	-760.0	1500.0	-760.0	28.0	10.0
8	1150.0	-750.0	1430.0	-750.0	47.0	10.0
9	4830.0	-1028.0	4804.0	-1000.0	76.0	15.0
10	4800.0	-999.0	4778.0	-1026.0	76.0	15.0

AIRCRAFT PARAMETERS ARE:

	SHPOS1			SHPOS2		
ID	X	Y	Z	X	Y	Z
1	2900.0	3300.0	12.0	2900.0	-3000.0	11.0

ID	SHACTP	SHVEL	SHANG
1	3	200.0	3.0

TABLE 3. MIDWAY RUNWAY 22L, CENTERLINE APPROACH FLIGHTPATH WAYPOINTS AND DATA

FLIGHTPATH TYPE: SEGMENTED
DATUM COORDINATES:
X: 4615. Y: 0. Z: 2.

TABLE OF FLIGHTPATH AND WAYPOINT DATA

WAYPT ID	X-COORD (FT)	Y-COORD (FT)	Z-COORD (FT)	VELOCITY (FT/SEC)	SAMPLING INCR (FT)	DISTANCE (NM) ALONG FP	FROM TH
1	43270.51	0.00	2441.01	200.00	40.00	7.13	-0.88
2	4626.11	0.00	9.71	200.00	40.00	13.51	-7.25
3	3750.00	0.00	11.00	200.00	40.00	13.65	-7.40
4	2950.00	0.00	13.00	200.00	40.00	13.78	-7.53
5	1375.00	0.00	18.00	200.00	40.00	14.04	-7.79
6	550.00	0.00	22.00	200.00	40.00	14.18	-7.92
7	0.00	0.00	22.00	200.00	40.00	14.27	-8.01

TABLE 4. MIDWAY RUNWAY 22L, ORBITAL FLIGHTPATH WAYPOINTS AND DATA

FLIGHTPATH TYPE: ORBIT
DATUM COORDINATES:
X: 4615. Y: 0. Z: 2.

ORBIT RADIUS (NM): 10.
ORBIT ELEVATION (FT): 964.

TABLE OF FLIGHTPATH AND WAYPOINT DATA

WAYPT ID	X-COORD (FT)	Y-COORD (FT)	Z-COORD (FT)	VELOCITY (FT/SEC)	SAMPLING INCR (FT)	DISTANCE (NM) ALONG FP	DISTANCE (NM) FROM TH
1	48096.30	43481.60	964.20	200.00	40.00	10.67	-10.67
2	50058.10	41427.10	964.20	200.00	40.00	11.14	-11.14
3	51922.80	39284.20	964.20	200.00	40.00	11.61	-11.61
4	53686.60	37057.40	964.20	200.00	40.00	12.07	-12.07
5	55345.70	34751.50	964.20	200.00	40.00	12.54	-12.54
6	56896.50	32371.50	964.20	200.00	40.00	13.01	-13.01
7	58335.70	29922.40	964.20	200.00	40.00	13.48	-13.48
8	59660.30	27409.50	964.20	200.00	40.00	13.94	-13.94
9	60867.50	24838.00	964.20	200.00	40.00	14.41	-14.41
10	61954.60	22213.60	964.20	200.00	40.00	14.88	-14.88
11	62919.30	19541.70	964.20	200.00	40.00	15.35	-15.35
12	63759.60	16828.20	964.20	200.00	40.00	15.82	-15.82
13	64473.60	14078.70	964.20	200.00	40.00	16.28	-16.28
14	65060.00	11299.20	964.20	200.00	40.00	16.75	-16.75
15	65517.30	8495.60	964.20	200.00	40.00	17.22	-17.22
16	65844.70	5673.80	964.20	200.00	40.00	17.69	-17.69
17	66041.40	2839.90	964.20	200.00	40.00	18.15	-18.15
18	66107.00	0.00	964.20	200.00	40.00	18.62	-18.62
19	66041.40	-2839.90	964.20	200.00	40.00	19.09	-19.09
20	65844.70	-5673.80	964.20	200.00	40.00	19.56	-19.56
21	65517.30	-8495.60	964.20	200.00	40.00	20.02	-20.02
22	65060.00	-11299.20	964.20	200.00	40.00	20.49	-20.49
23	64473.60	-14078.70	964.20	200.00	40.00	20.96	-20.96
24	63759.60	-16828.20	964.20	200.00	40.00	21.43	-21.43
25	62919.30	-19541.70	964.20	200.00	40.00	21.89	-21.89
26	61954.60	-22213.60	964.20	200.00	40.00	22.36	-22.36
27	60867.50	-24838.00	964.20	200.00	40.00	22.83	-22.83
28	59660.30	-27409.50	964.20	200.00	40.00	23.30	-23.30
29	58335.80	-29922.40	964.20	200.00	40.00	23.76	-23.76
30	56896.50	-32371.50	964.20	200.00	40.00	24.23	-24.23
31	55345.70	-34751.50	964.20	200.00	40.00	24.70	-24.70
32	53686.60	-37057.40	964.20	200.00	40.00	25.17	-25.17
33	51922.80	-39284.20	964.20	200.00	40.00	25.63	-25.63
34	50058.10	-41427.10	964.20	200.00	40.00	26.10	-26.10
35	48096.30	-43481.60	964.20	200.00	40.00	26.57	-26.57

TABLE 5. MIDWAY RUNWAY 22L, MULTIPATH RANKINGS FOR CENTERLINE APPROACH FLIGHTPATH

AIRCRAFT & BUILDING MULTIPATH AMPLITUDE RANKINGS

******* AZIMUTH SYSTEM *******

OBST ID	RANK	MLTPATH AMP(DB)	X-AXIS REF
GRND 0	21	-80.00	6.254
BLDG 1	17	-53.58	4.233
BLDG 2	18	-60.00	4.628
BLDG 3	19	-60.00	4.990
BLDG 4	15	-27.63	1.257
BLDG 5	4	5.56	-0.349
BLDG 6	3	-3.89	-0.053
BLDG 7	2	-0.84	-0.342
BLDG 8	1	0.74	-0.435
BLDG 9	20	-60.00	-0.395
BLDG 10	6	-14.52	-0.165
ACFT 3	11	-21.62	0.026
ACFT 4	8	17.66	-0.059
ACFT 5	14	-20.8[illegible]	-0.152
ACFT 6	10	[illegible]	0.033
ACFT 7	5	[illegible]	-0.079
ACFT 8	13	[illegible]	-0.105
ACFT 9	9	[illegible]	0.152
ACFT 10	16	[illegible]	0.685
ACFT 12	12	[illegible]	0.171
ACFT 15	7	[illegible]	0.586

AIRCRAFT & BUILDING MULTIPATH AMPLITUDE RANKINGS

******* DME/F SYSTEM *******

OBST ID	RANK	MLTPATH AMP(DB)	X-AXIS REF
GRND 0	21	-80.00	6.254
BLDG 1	17	-50.46	0.276
BLDG 2	16	-50.46	1.909
BLDG 3	19	-53.98	-0.158
BLDG 4	15	-28.40	0.118
BLDG 5	4	-4.60	-0.349
BLDG 6	1	-1.09	-0.053
BLDG 7	3	-3.15	-0.342
BLDG 8	2	-1.56	-0.375
BLDG 9	20	-53.98	-0.402
BLDG 10	5	-10.52	-0.165
ACFT 3	11	-22.38	-0.020
ACFT 4	12	-23.74	-0.053
ACFT 5	14	-24.58	-0.152
ACFT 6	7	-16.71	-0.046
ACFT 7	8	-17.72	-0.079
ACFT 8	10	-19.91	-0.099
ACFT 9	13	-24.29	-0.408
ACFT 10	18	-28.64	-0.685
ACFT 12	9	-19.74	-0.184
ACFT 15	6	-16.48	-0.599

AIRCRAFT & BUILDING MULTIPATH AMPLITUDE RANKING

******* ELEVATION SYSTEM *******

OBST ID	RANK	MLTPATH AMP(DB)	X-AXIS REF
GRND 0	21	-80.00	6.254
BLDG 1	2	-3.21	-0.558
BLDG 2	3	-3.62	-0.593
BLDG 3	4	-15.60	-0.310
BLDG 4	8	-24.88	2.133
BLDG 5	15	-47.96	-0.869
BLDG 6	1	-1.34	-0.836
BLDG 7	12	-33.98	-0.882
BLDG 8	13	-34.89	-0.869
BLDG 9	14	-37.72	2.745
BLDG 10	16	-47.96	-0.843
ACFT 3	7	-20.18	-0.046
ACFT 4	18	-60.00	0.105
ACFT 5	19	-60.00	0.020
ACFT 6	6	-19.09	-0.066
ACFT 7	9	-26.38	-0.882
ACFT 8	10	-26.74	-0.770
ACFT 9	5	-17.65	-0.777
ACFT 10	11	-31.37	-0.362
ACFT 12	20	-60.00	-0.843
ACFT 15	17	-53.96	-0.869

TABLE 6. MIDWAY RUNWAY 22L, MULTIPATH RANKINGS FOR ORBITAL FLIGHTPATH

AIRCRAFT & BUILDING MULTIPATH AMPLITUDE RANKINGS

******* AZIMUTH SYSTEM *******				******* DME/P SYSTEM *******				******* ELEVATION SYSTEM *******			
OBST ID	RANK	MLTPATH AMP(DB)	X-AXIS REF	OBST ID	RANK	MLTPATH AMP(DB)	X-AXIS REF	OBST ID	RANK	MLTPATH AMP(DB)	X-AXIS REF
GRND 0	17	-80.00	-41.900	GRND 0	17	-80.00	-41.000	GRND 0	17	-80.00	-41.900
BLDG 1	3	-3.74	-41.900	BLDG 1	5	-16.83	-41.311	BLDG 1	9	-53.98	41.923
BLDG 2	4	-12.80	-41.600	BLDG 2	4	-16.77	-41.733	BLDG 2	5	-50.46	41.677
BLDG 3	5	-14.85	-41.451	BLDG 3	6	-18.34	-40.054	BLDG 3	10	-53.98	41.747
BLDG 4	6	-15.30	2.646	BLDG 4	3	-13.56	2.008	BLDG 4	2	-2.82	1.232
BLDG 5	18	-80.00	41.888	BLDG 5	18	-80.00	41.923	BLDG 5	18	-80.00	41.923
BLDG 6	19	-80.00	41.923	BLDG 6	19	-80.00	41.747	BLDG 6	19	-80.00	41.466
BLDG 7	2	1.73	-21.490	BLDG 7	2	-9.40	-21.742	BLDG 7	11	-60.00	-41.600
BLDG 8	1	3.23	-24.830	BLDG 8	1	-3.16	-24.448	BLDG 8	6	-50.46	-24.890
BLDG 9	20	-80.00	-41.900	BLDG 9	20	-80.00	-41.900	BLDG 9	1	3.09	12.680
BLDG 10	21	-80.00	-41.900	BLDG 10	21	-80.00	-41.900	BLDG 10	20	-80.00	-41.900
ACFT 3	10	-50.46	-6.357	ACFT 3	11	-50.46	-6.184	ACFT 3	7	-50.46	-15.648
ACFT 4	16	-53.98	1.921	ACFT 4	12	-50.46	1.783	ACFT 4	4	-47.96	10.227
ACFT 5	11	-50.46	2.107	ACFT 5	13	-50.46	2.050	ACFT 5	8	-50.46	20.922
ACFT 6	12	-50.46	4.267	ACFT 6	14	-50.46	4.108	ACFT 6	21	-80.00	-41.900
ACFT 7	9	-47.96	5.750	ACFT 7	15	-50.46	5.681	ACFT 7	12	-60.00	-41.240
ACFT 8	13	-50.46	8.200	ACFT 8	16	-50.46	8.407	ACFT 8	13	-60.00	-41.900
ACFT 9	8	-23.61	-8.669	ACFT 9	8	-30.17	-9.187	ACFT 9	14	-60.00	-1.070
ACFT 10	14	-50.46	-4.528	ACFT 10	9	-47.96	-3.769	ACFT 10	3	-25.19	2.439
ACFT 12	15	-50.46	5.612	ACFT 12	10	-47.96	5.543	ACFT 12	15	-60.00	-41.311
ACFT 15	7	-19.17	-20.425	ACFT 15	7	-20.82	-20.459	ACFT 15	16	-60.00	-1.010

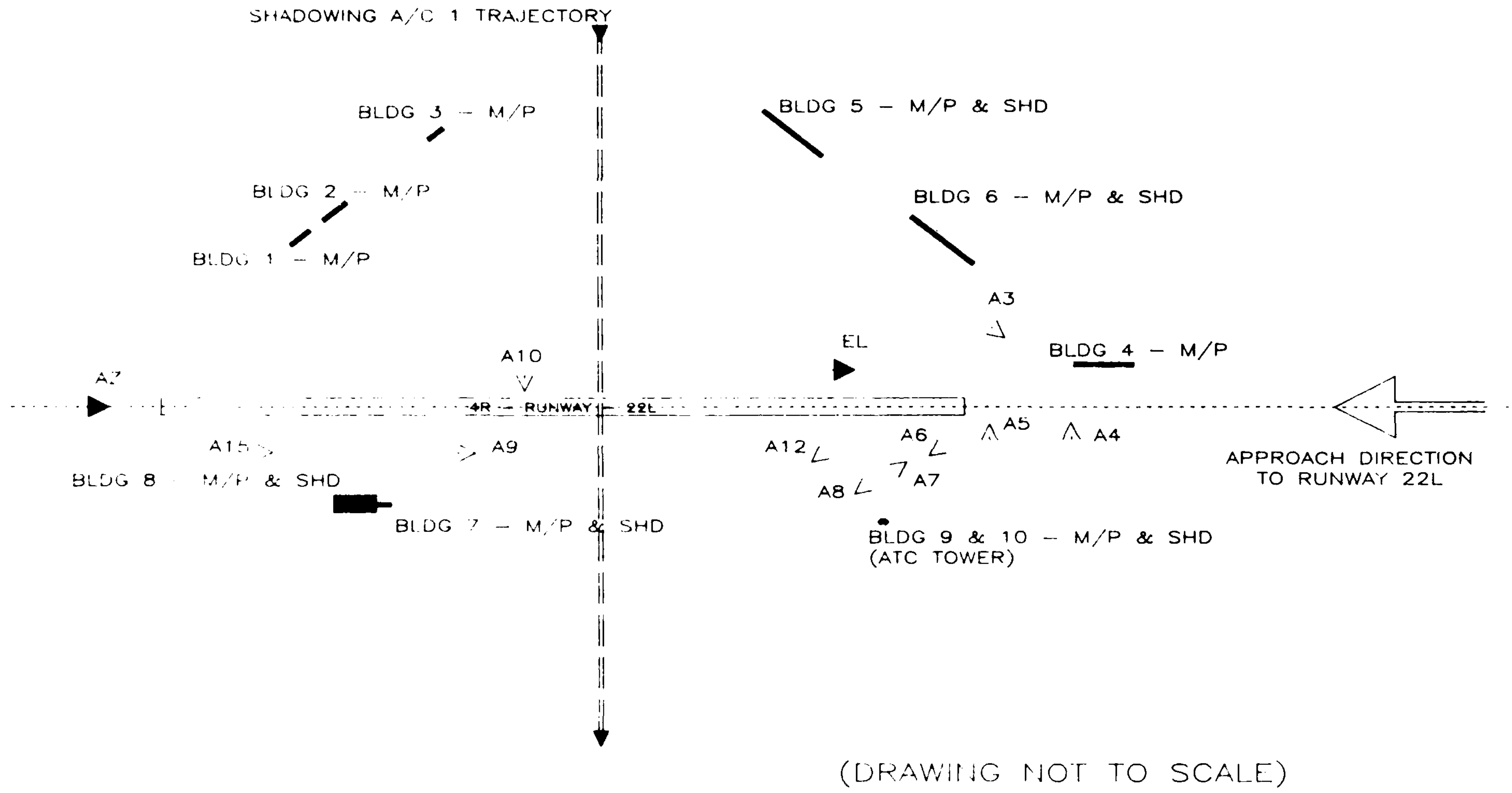

FIGURE 1 MIDWAY RUNWAY 22L, SCENARIO MAP

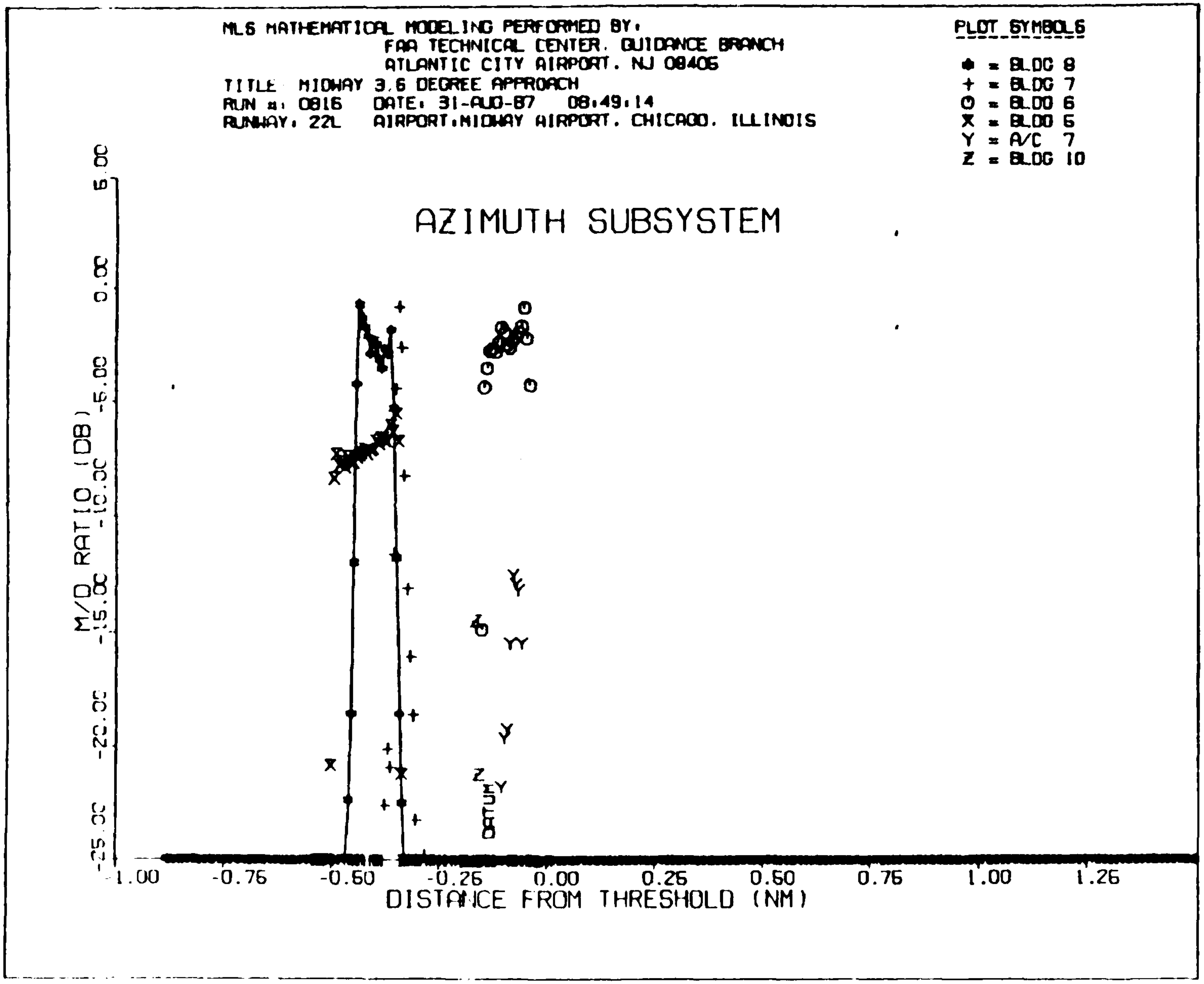

FIGURE 2 -- MIDWAY RUNWAY 22L, APPROACH FLIGHTPATH, AZIMUTH SUBSYSTEM, MULTIPATH/DIRECT SIGNAL RATIO PLOT.

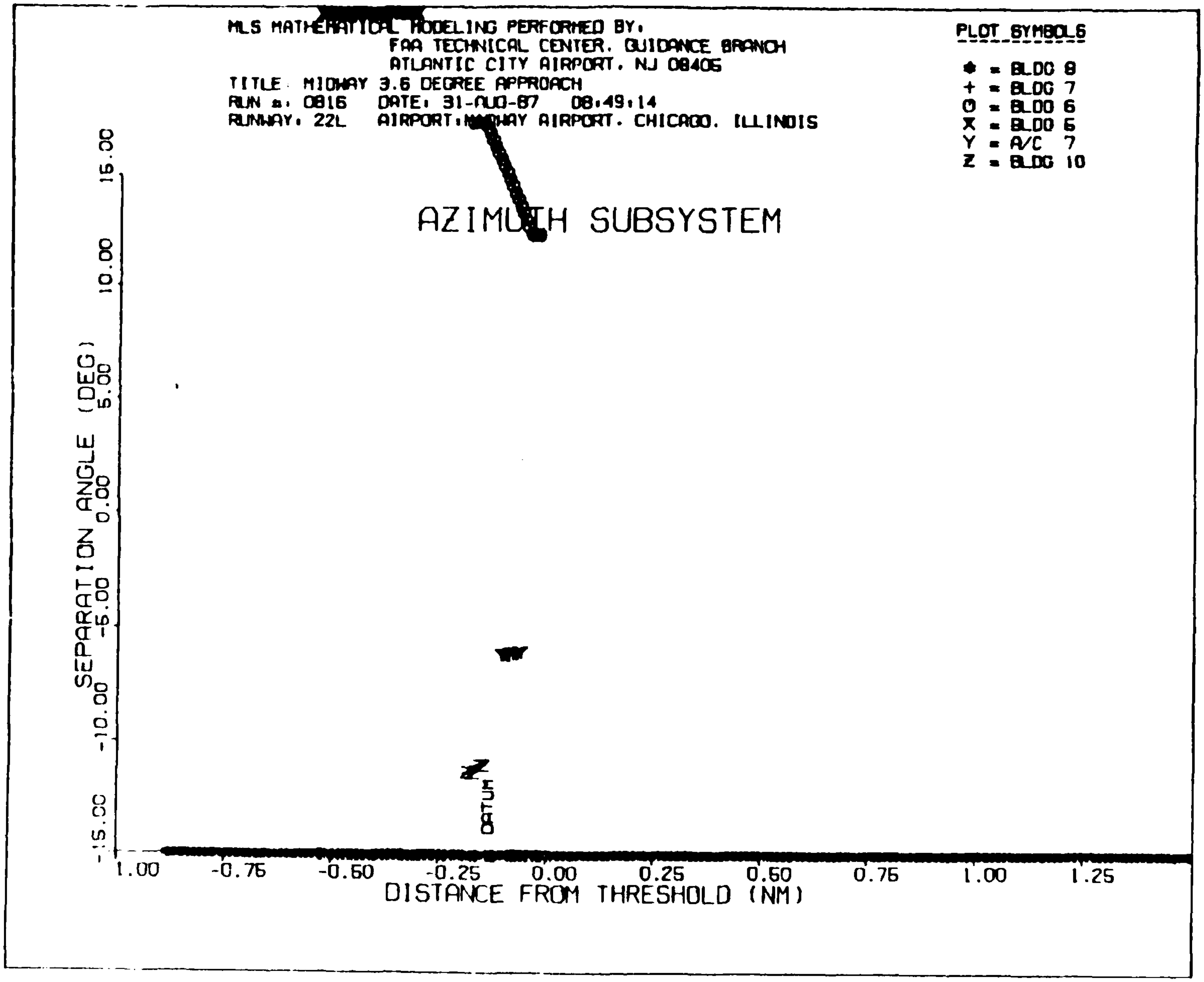

FIGURE 3 - MIDWAY RUNWAY 22L, APPROACH FLIGHTPATH, AZIMUTH SUBSYSTEM, SEPARATION ANGLE PLOT.

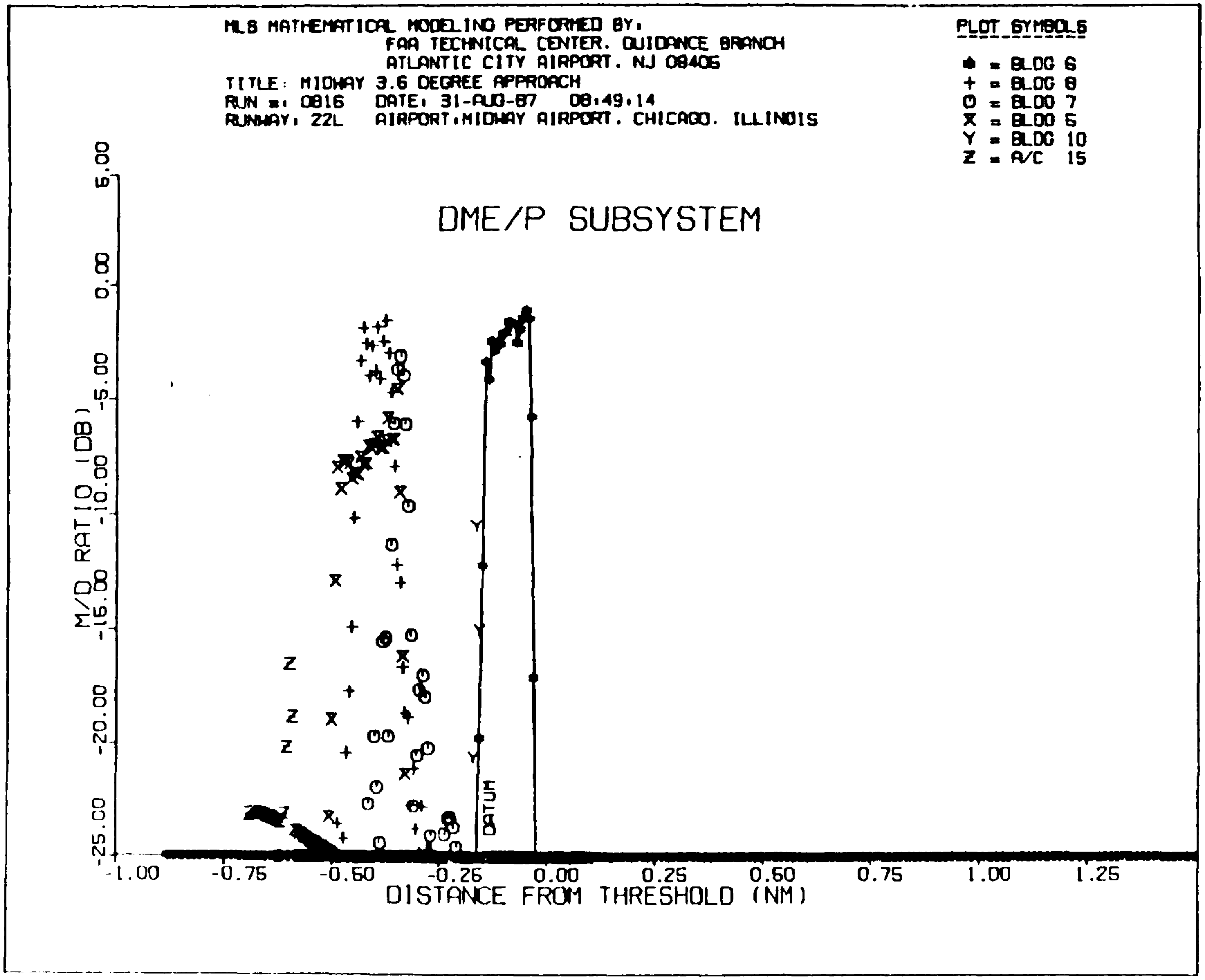

FIGURE 4 - MIDWAY RUNWAY 22L, APPROACH FLIGHTPATH, DME/P SUBSYSTEM, MULTIPATH/DIRECT SIGNAL RATIO PLOT.

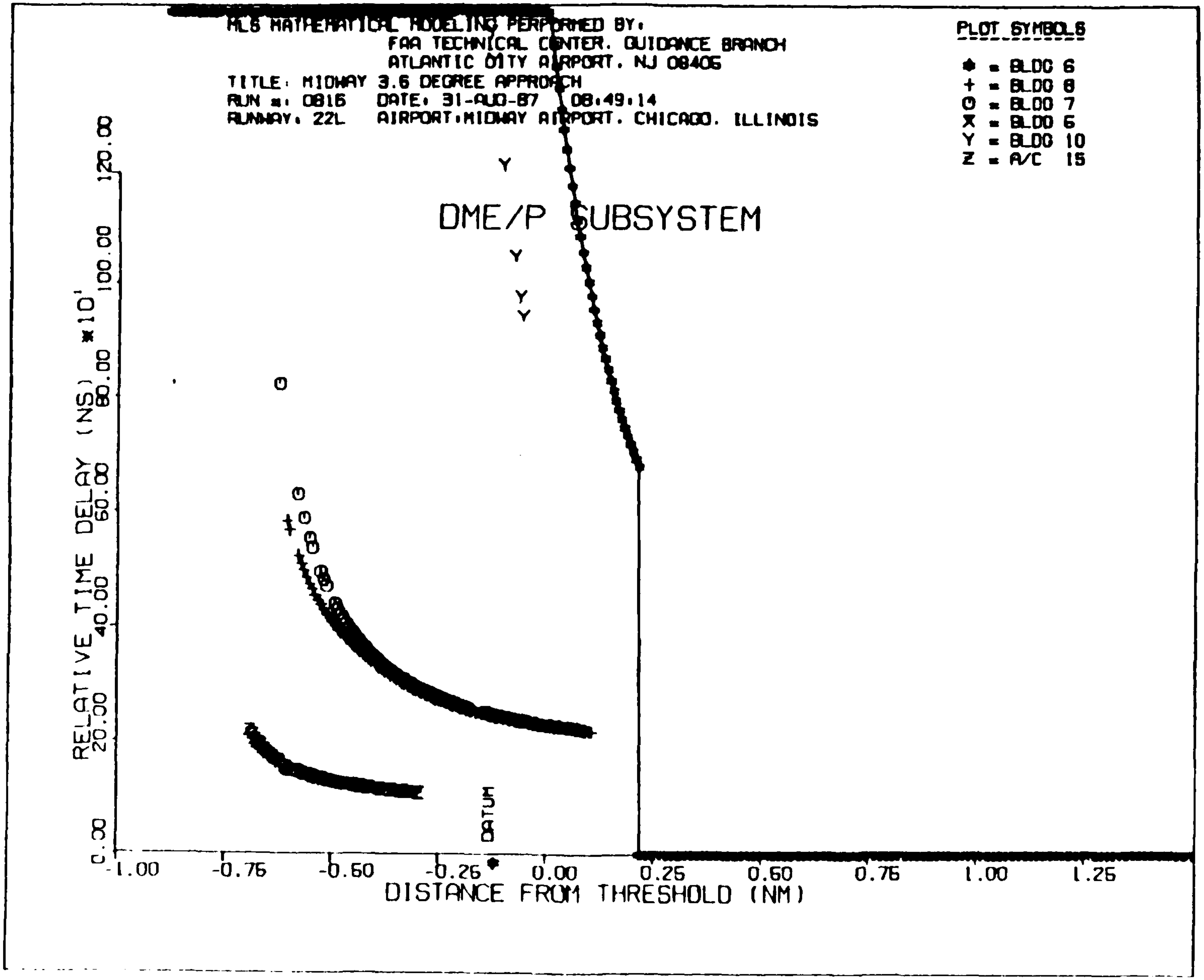

FIGURE 5 - MIDWAY RUNWAY 22L, APPROACH FLIGHTPATH, DME/P SUBSYSTEM, RELATIVE TIME DELAY PLOT.

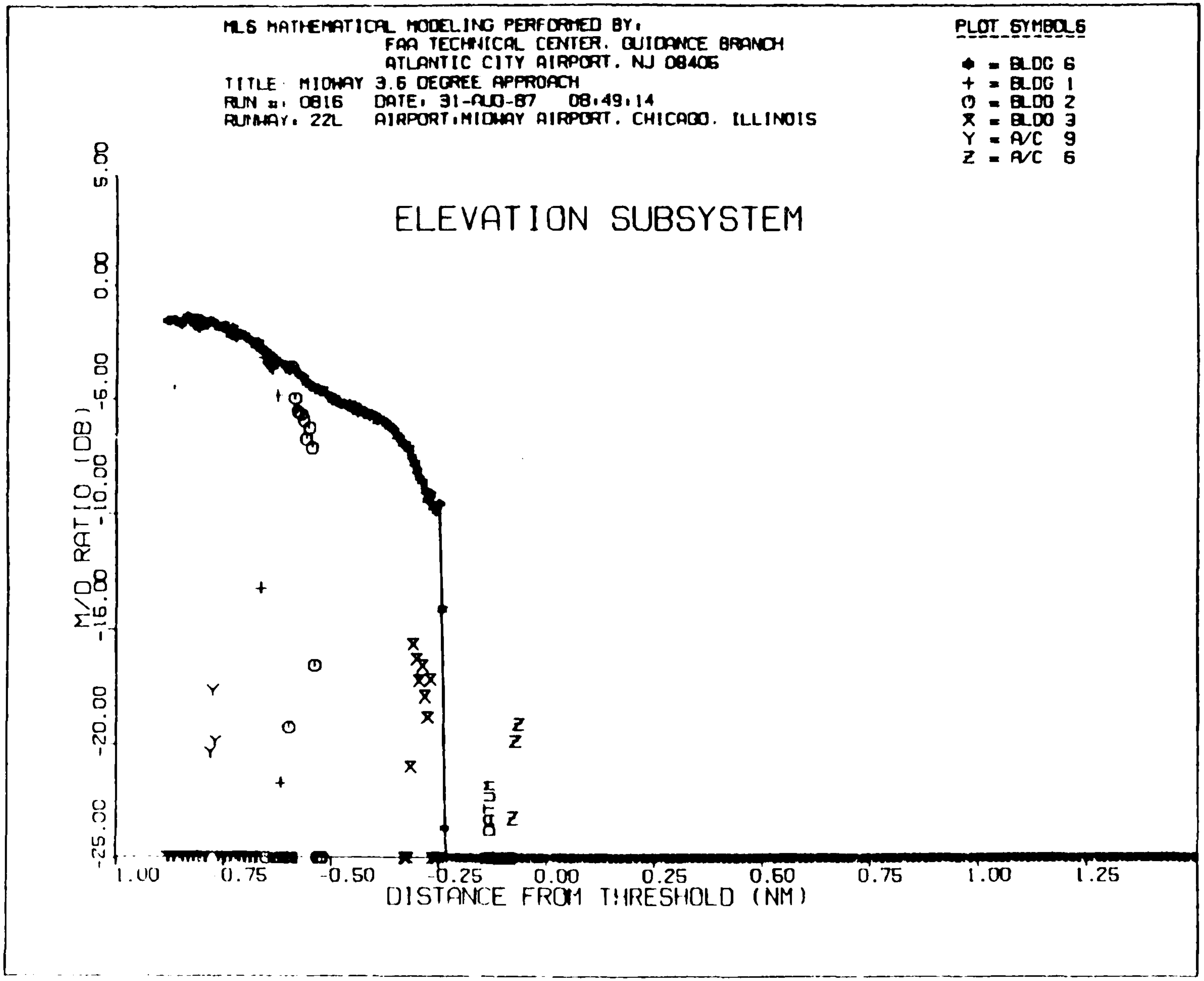

FIGURE 6 - MIDWAY RUNWAY 22L, APPROACH FLIGHTPATH, ELEVATION SUBSYSTEM, MULTIPATH/DIRECT SIGNAL RATIO PLOT.

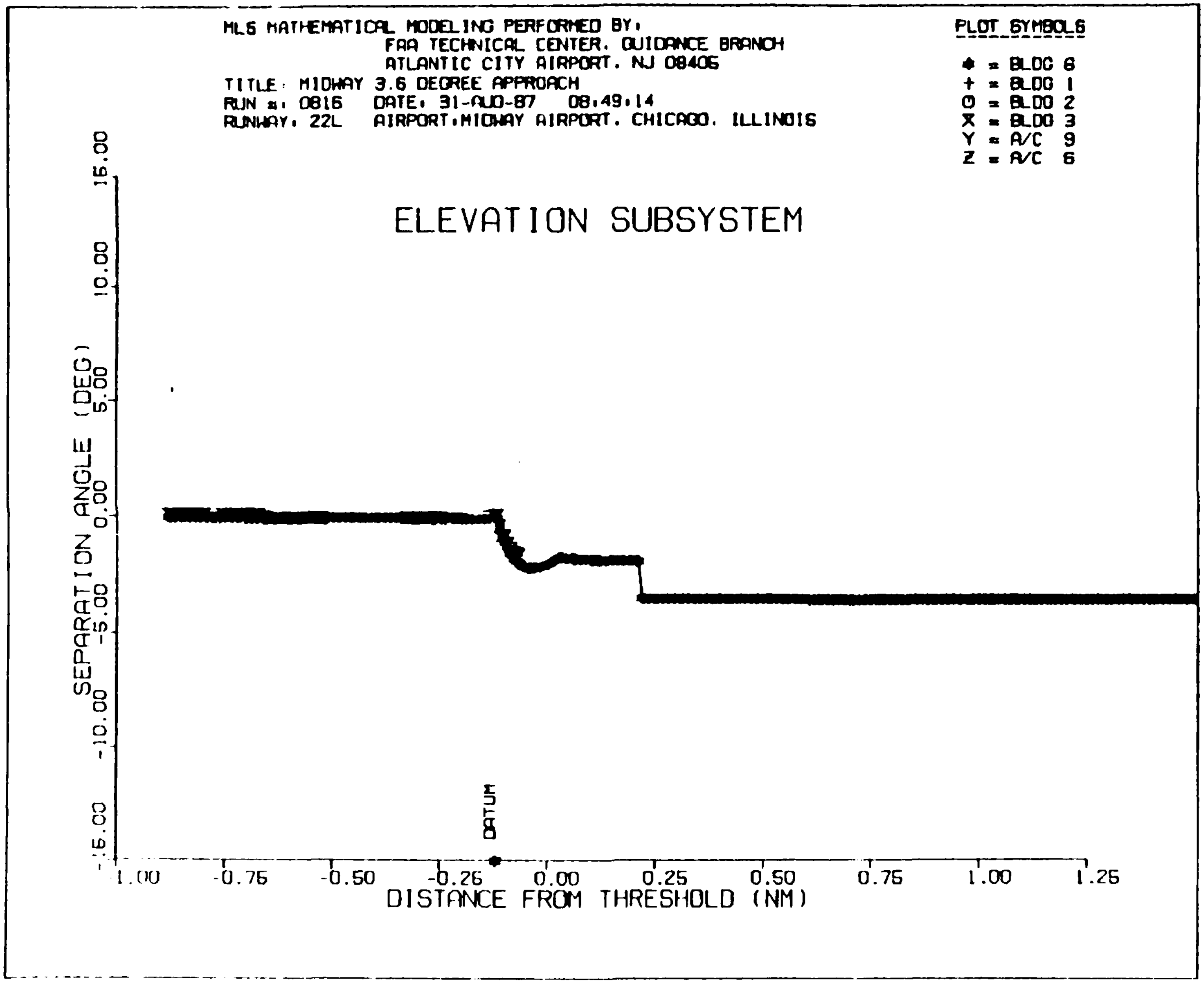

FIGURE 7 - MIDWAY RUNWAY 22L, APPROACH FLIGHTPATH, ELEVATION SUBSYSTEM, SEPARATION ANGLE PLOT.

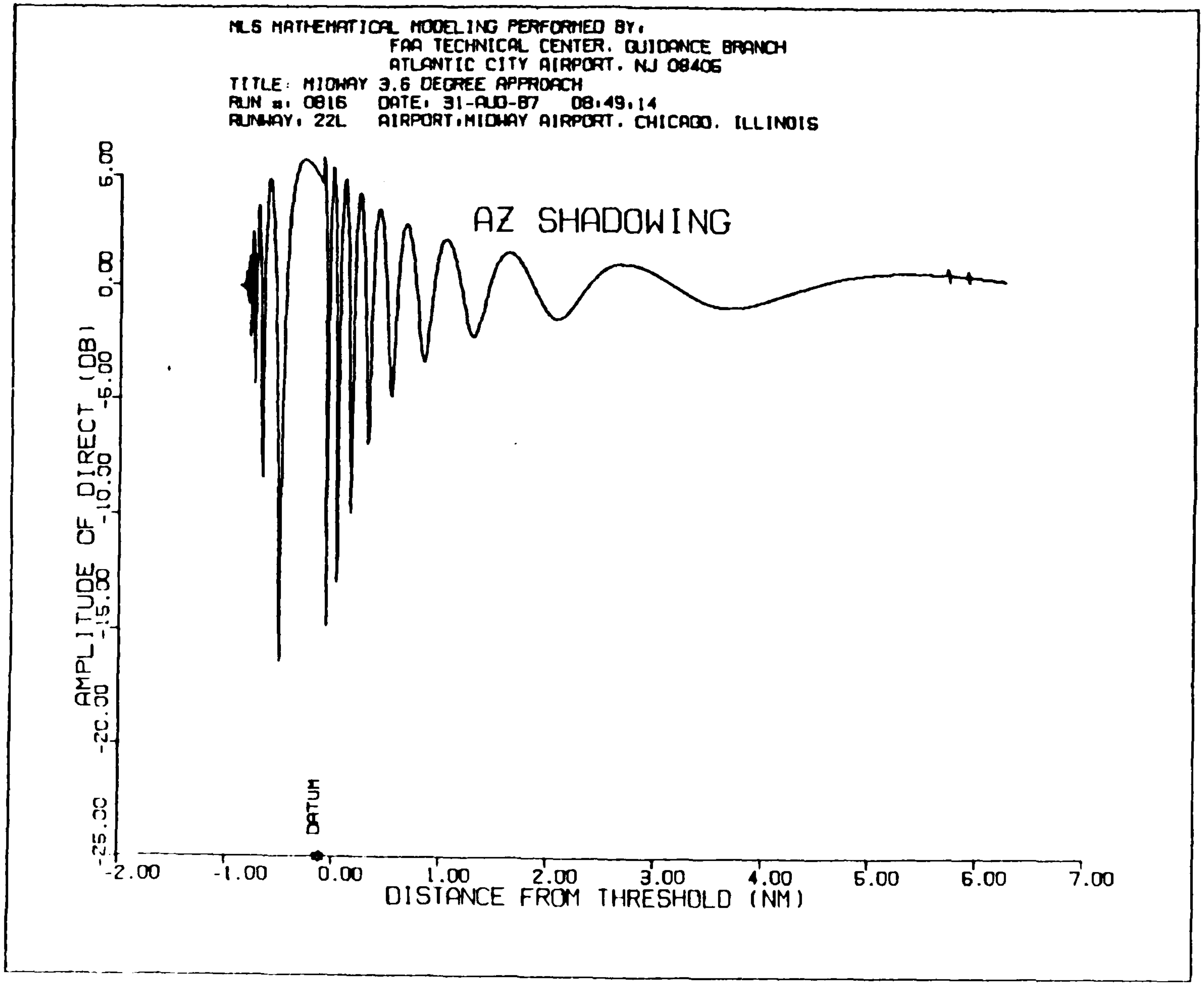

FIGURE 8 -- MIDWAY RUNWAY 22L, APPROACH FLIGHTPATH, AZIMUTH SUBSYSTEM, SHADOWING PLOT.

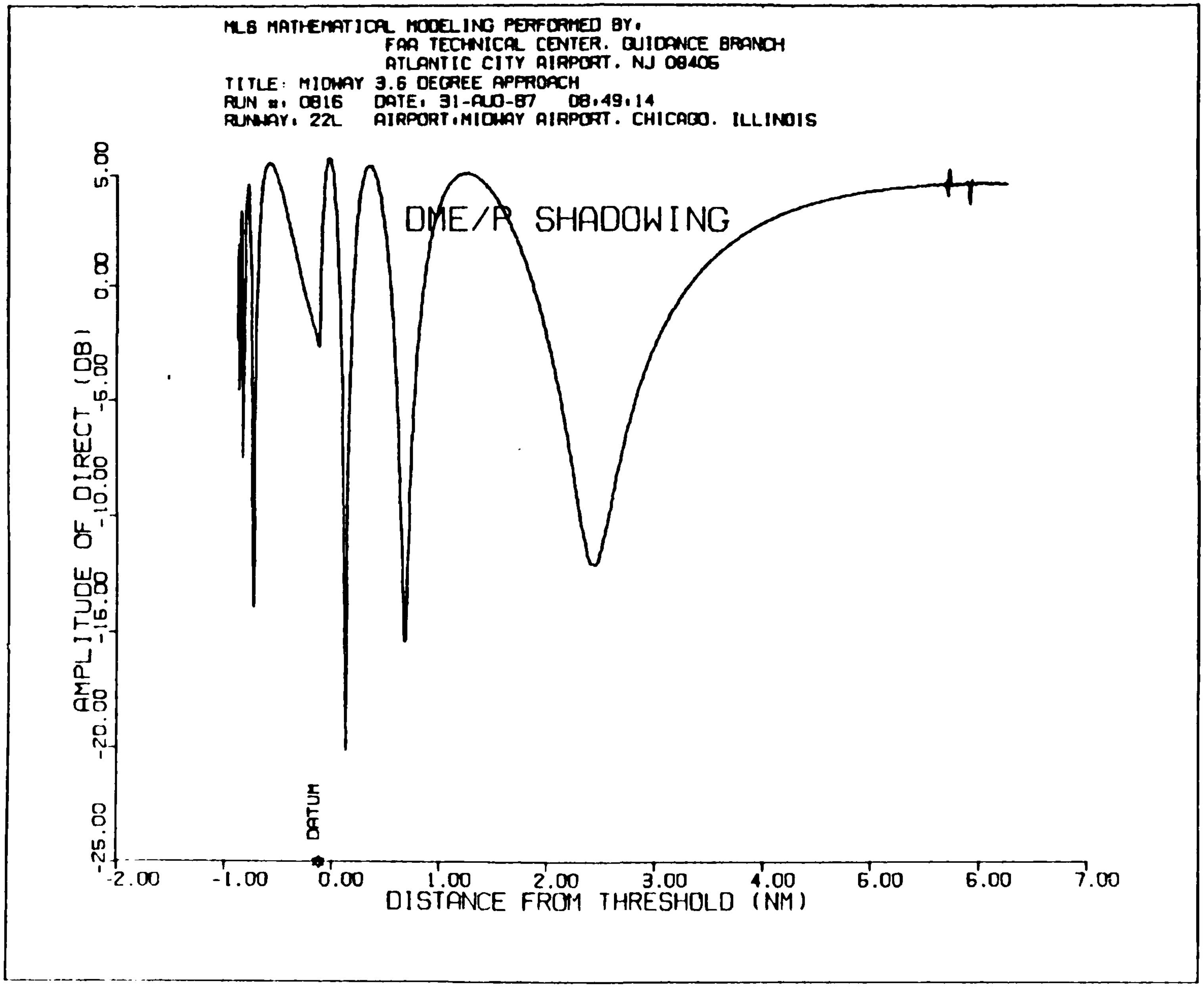

FIGURE 9 - MIDWAY RUNWAY 22L, APPROACH FLIGHTPATH, DME/P SUBSYSTEM, SHADOWING PLOT.

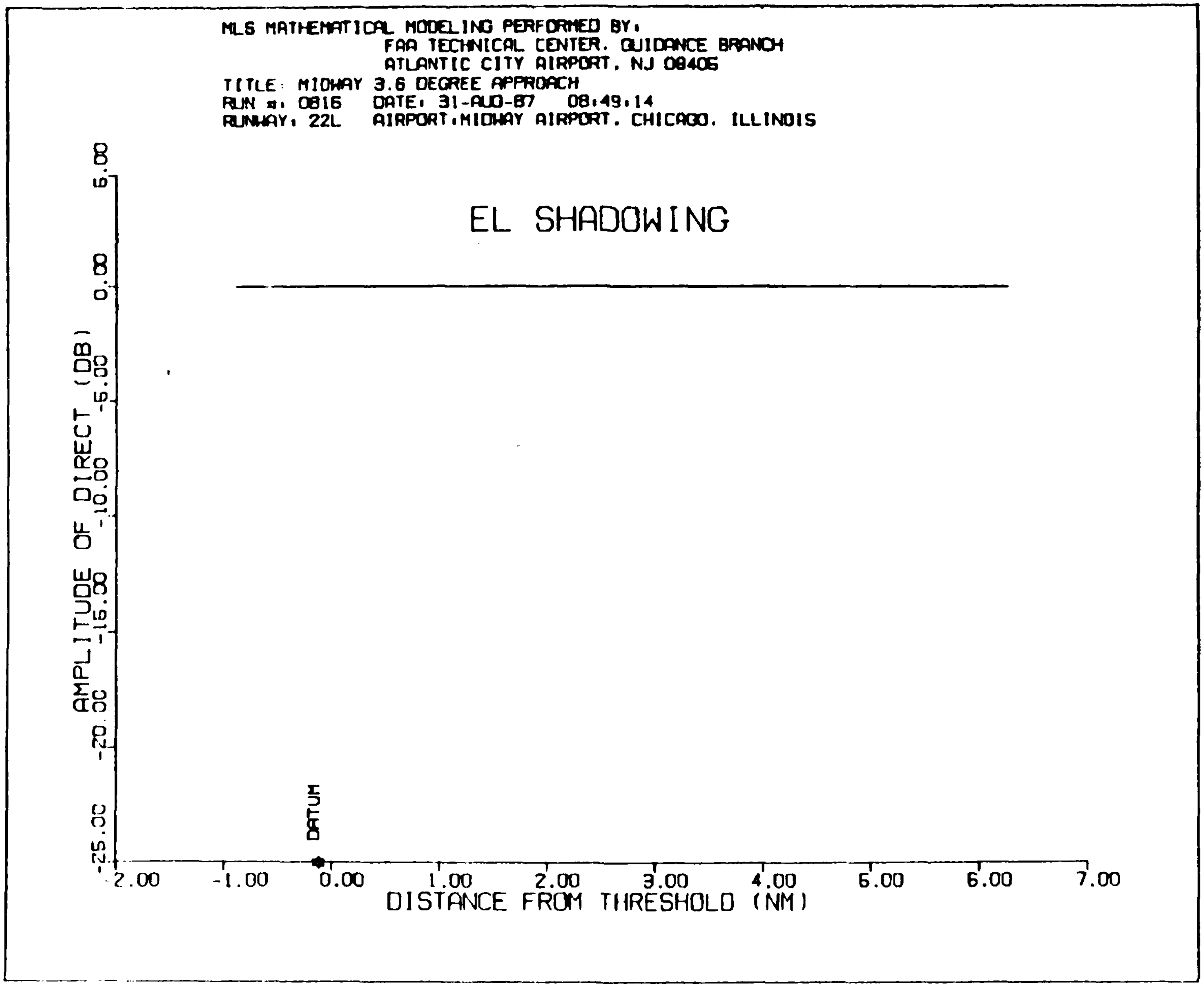

FIGURE 10 - MIDWAY RUNWAY 22L, APPROACH FLIGHTPATH, ELEVATION SUBSYSTEM, SHADOWING PLOT.

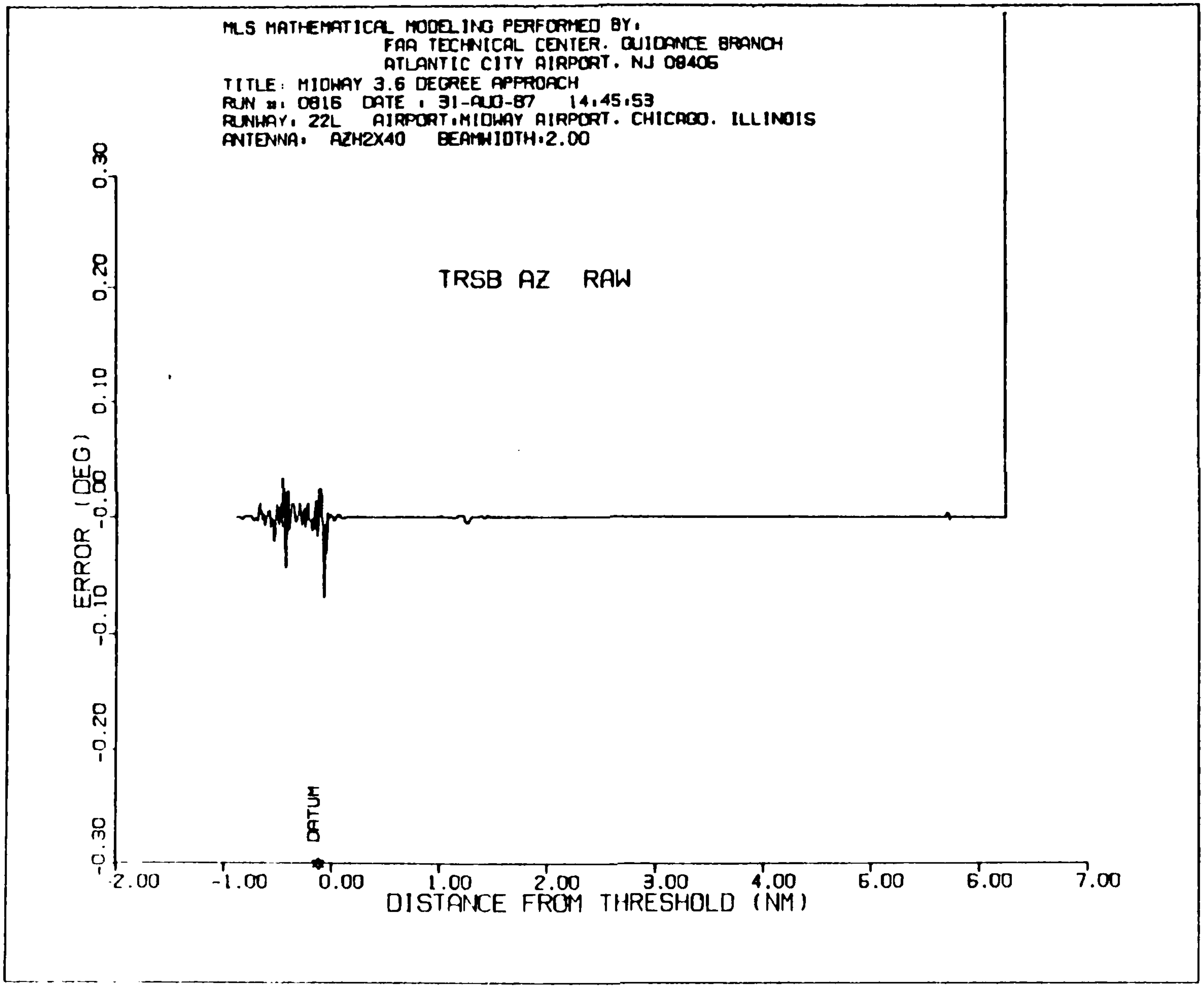

FIGURE 11 - MIDWAY RUNWAY 22L, APPROACH FLIGHTPATH, AZIMUTH SUBSYSTEM, RAW ERROR PLOT.

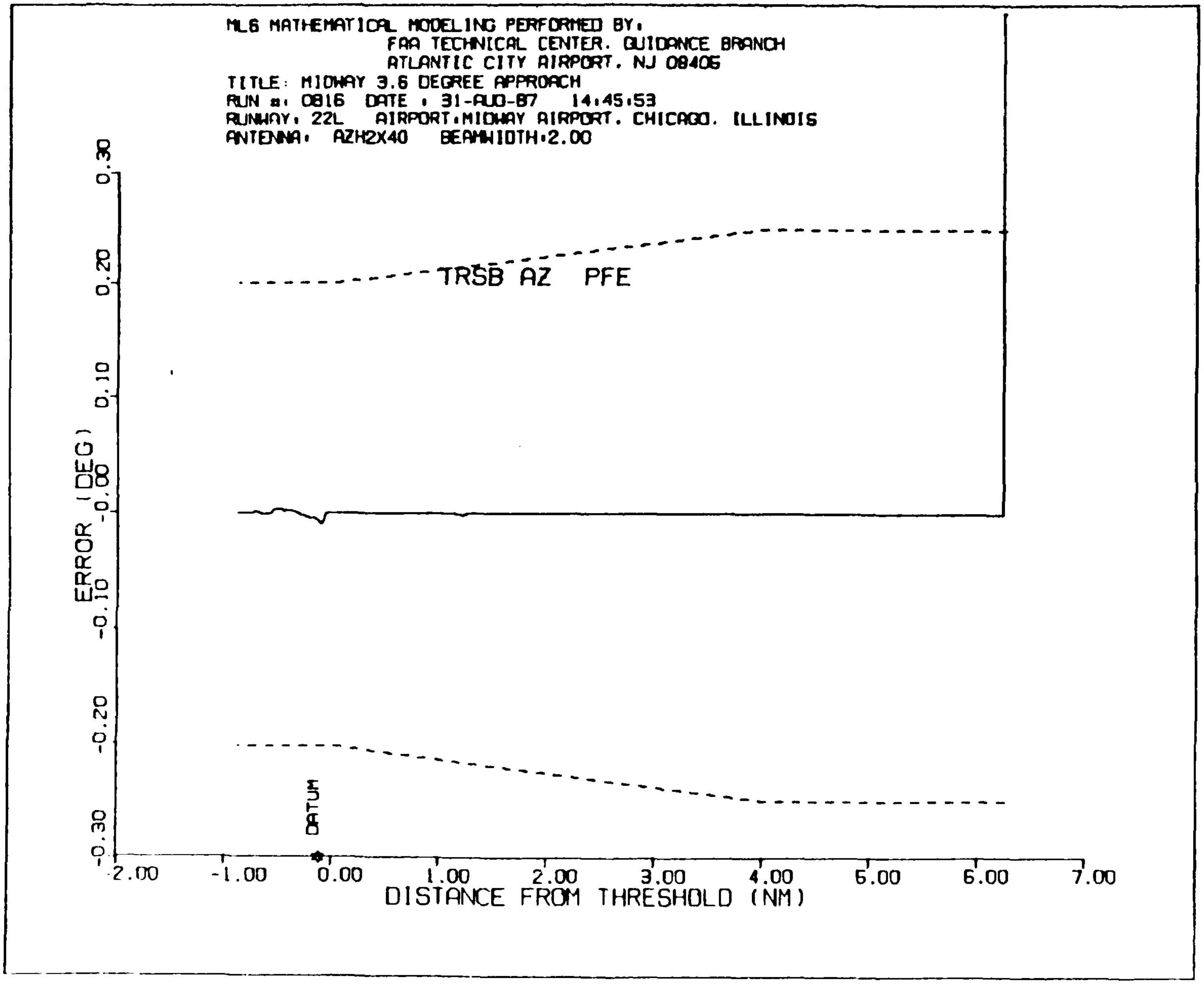

FIGURE 12 - MIDWAY RUNWAY 22L, APPROACH FLIGHTPATH, AZIMUTH SUBSYSTEM, PFE FILTERED PLOT.

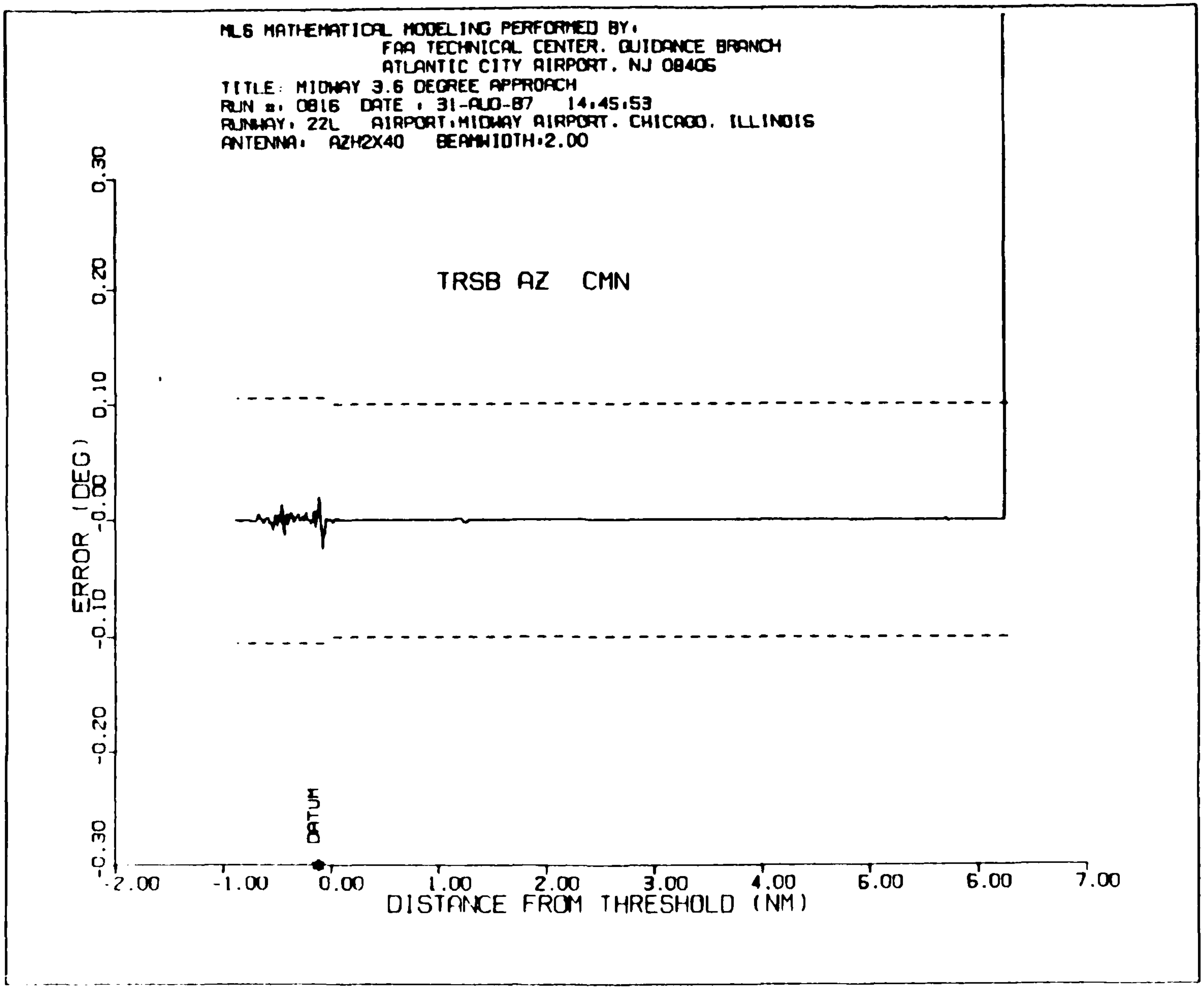

FIGURE 13 - MIDWAY RUNWAY 22L, APPROACH FLIGHTPATH, AZIMUTH SUBSYSTEM, CMN FILTERED PLOT.

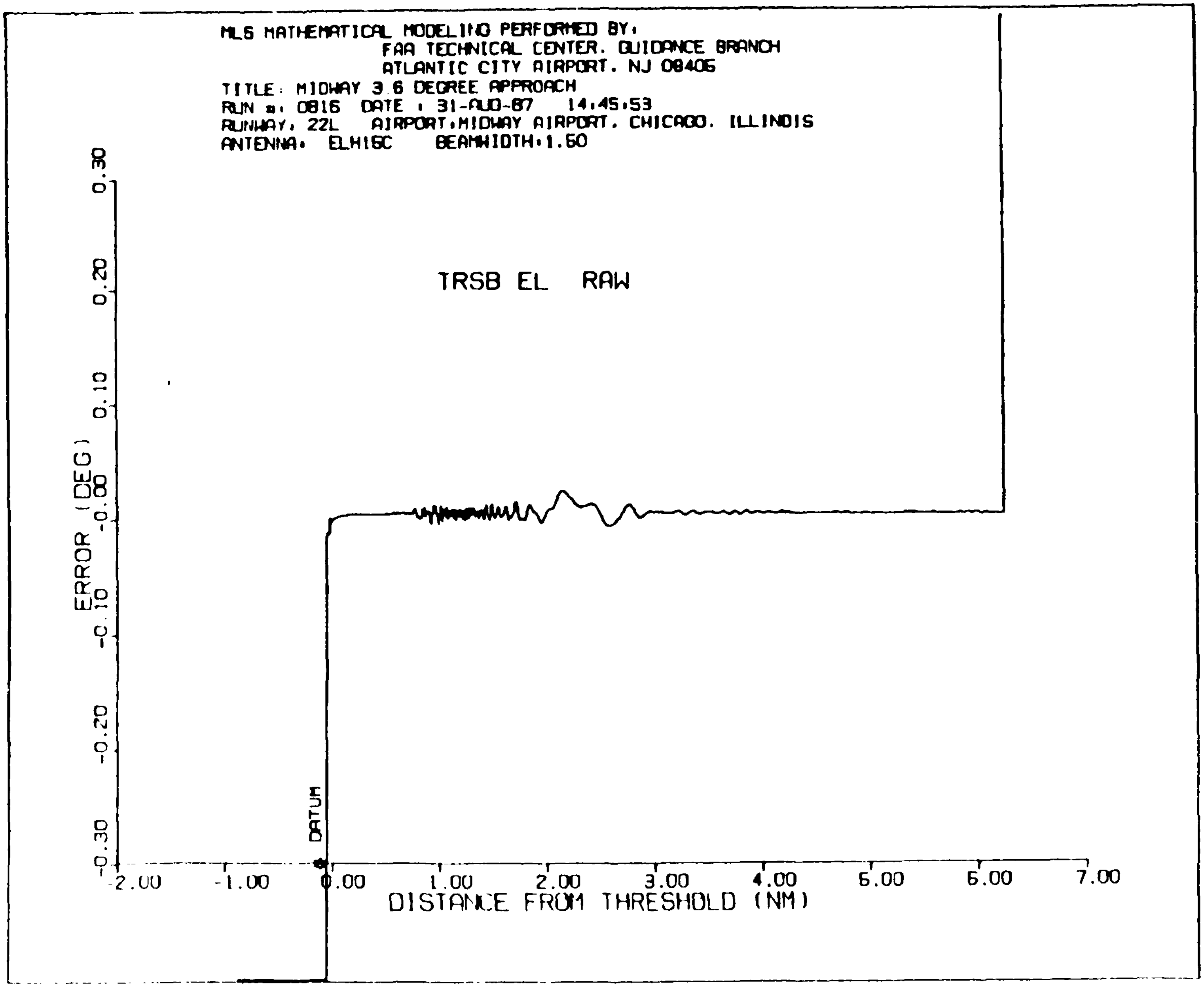

FIGURE 14 - MIDWAY RUNWAY 22L, APPROACH FLIGHTPATH, ELEVATION SUBSYSTEM, RAW ERROR PLOT.

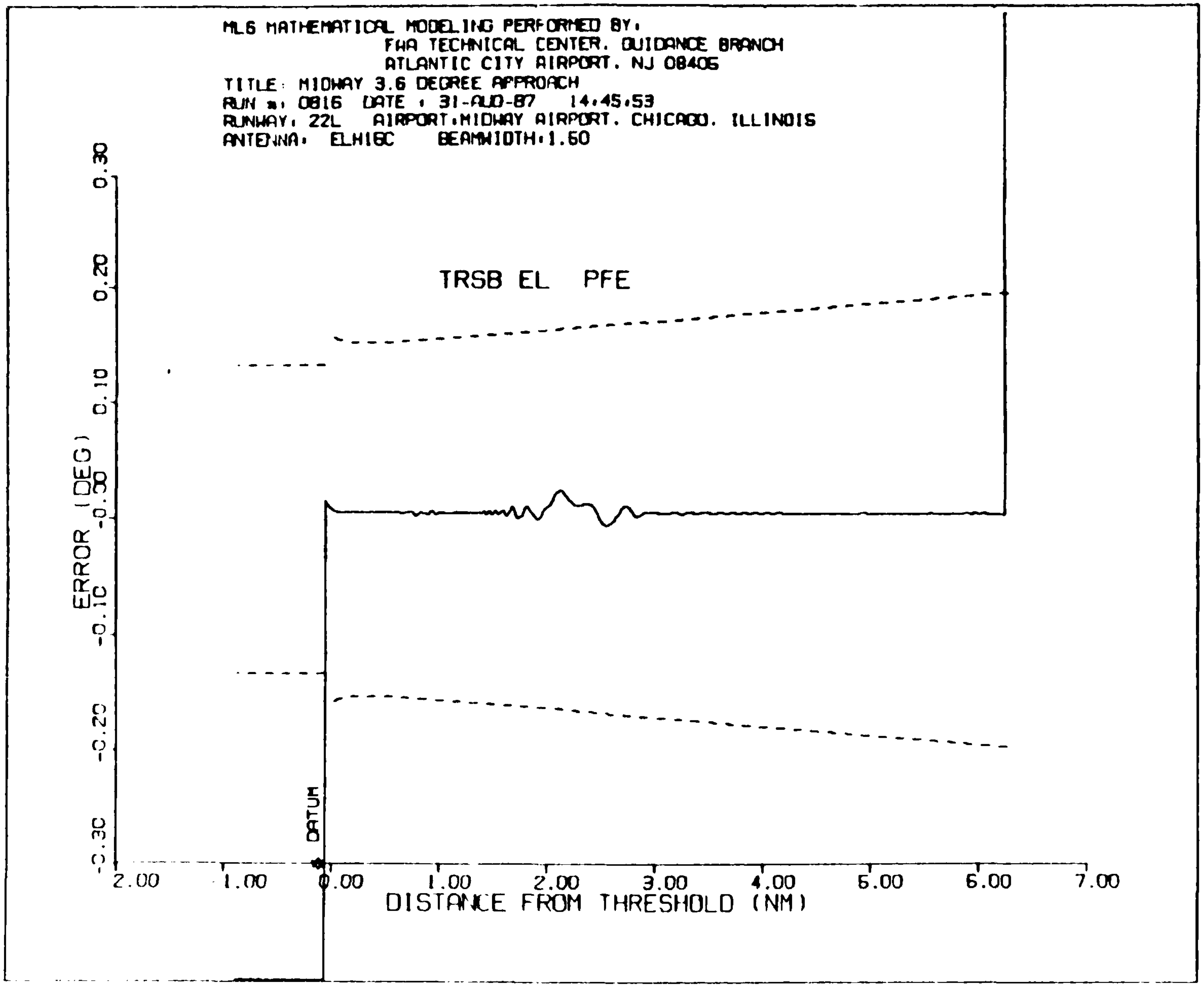

FIGURE 15. MIDWAY RUNWAY 22L APPROACH FLIGHTPATH, ELEVATION SUBSYSTEM, PFE FILTERED PLOT.

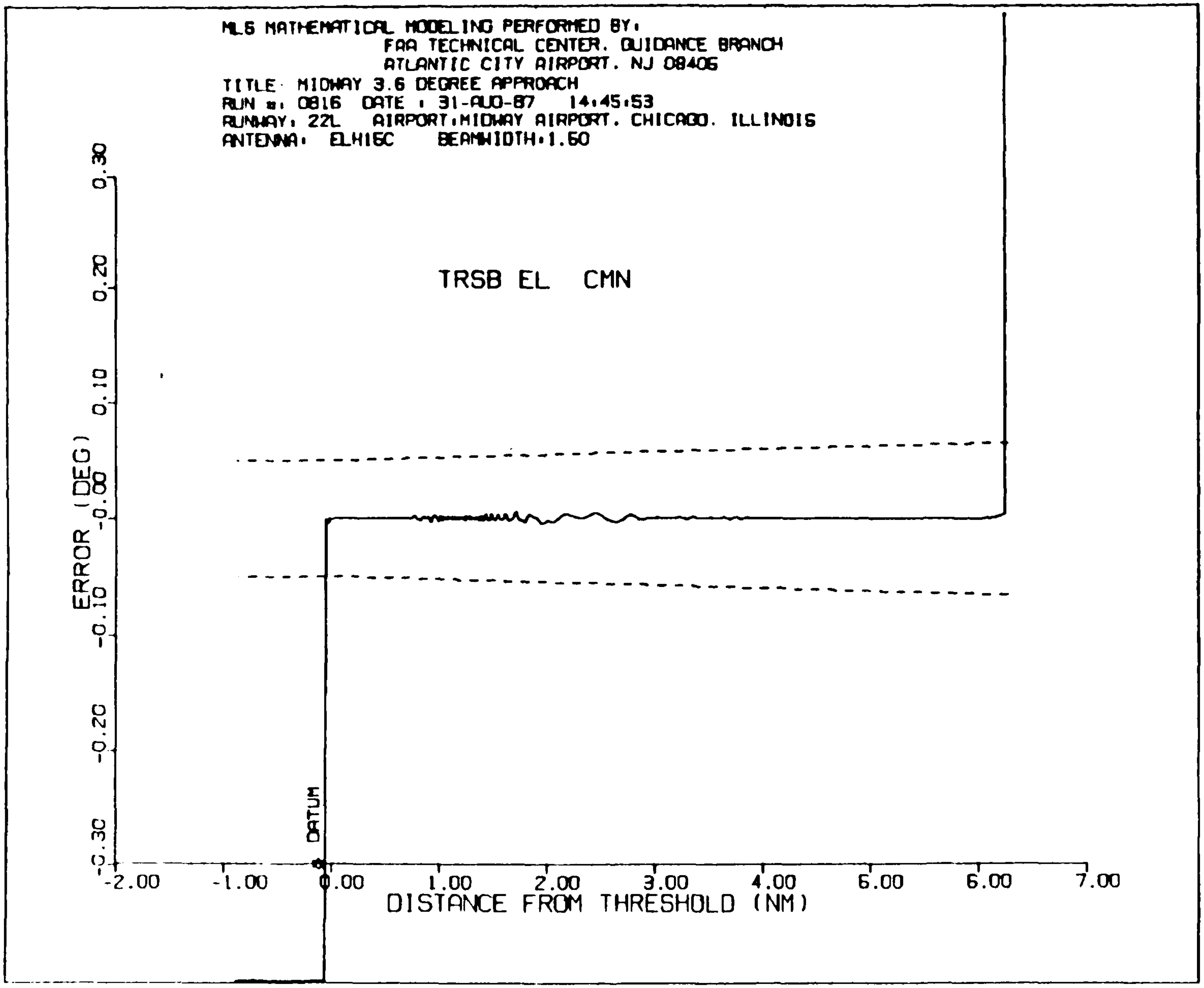

FIGURE 16 - MIDWAY RUNWAY 22L, APPROACH FLIGHTPATH, ELEVATION SUBSYSTEM, CMN FILTERED PLOT.

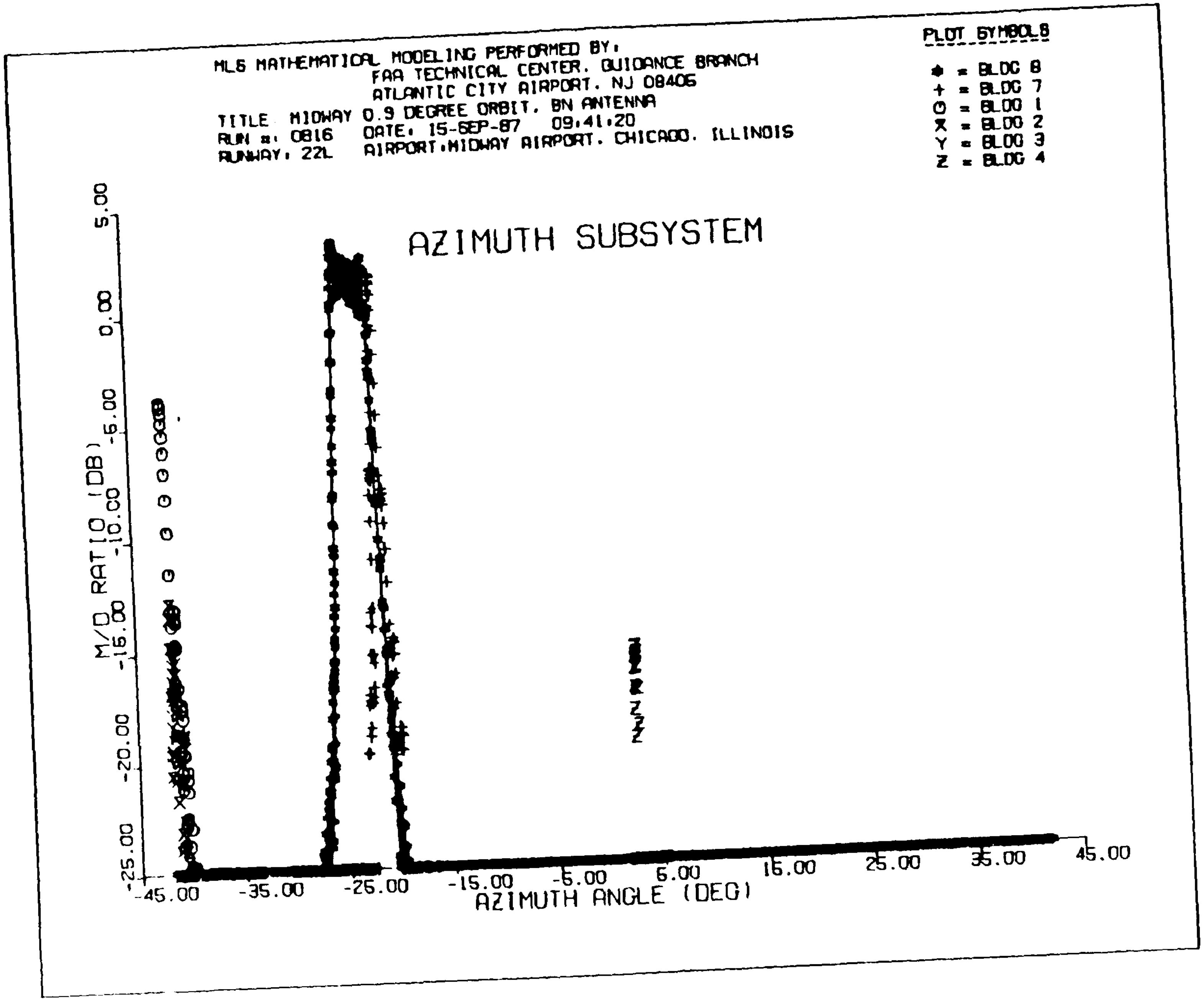

FIGURE 17 - MIDWAY RUNWAY 22L, ORBITAL FLIGHTPATH, AZIMUTH SUBSYSTEM, MULTIPATH/DIRECT SIGNAL RATIO PLOT.

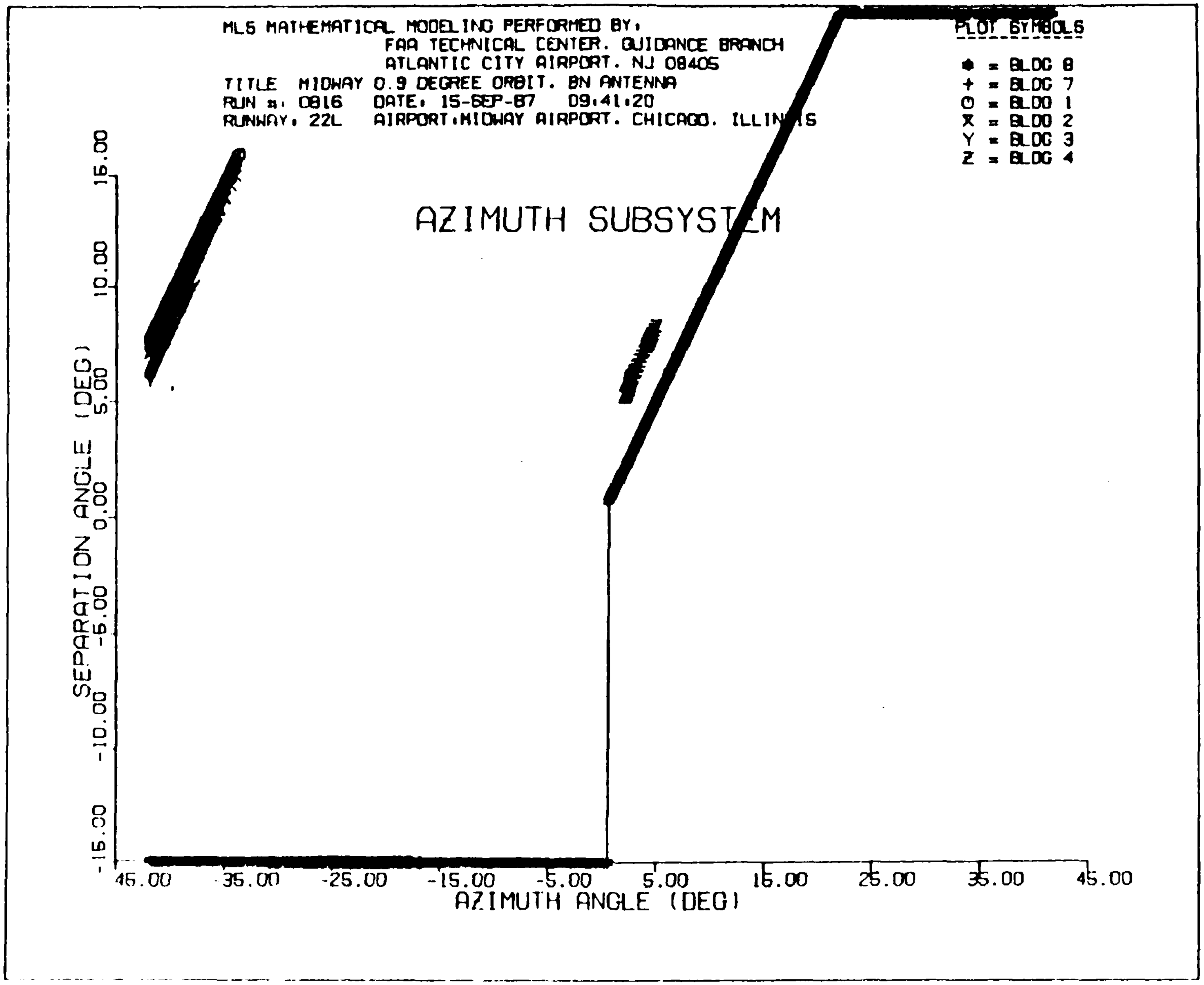

FIGURE 18 -- MIDWAY RUNWAY 22L, ORBITAL FLIGHTPATH, AZIMUTH SUBSYSTEM, SEPARATION ANGLE PLOT.

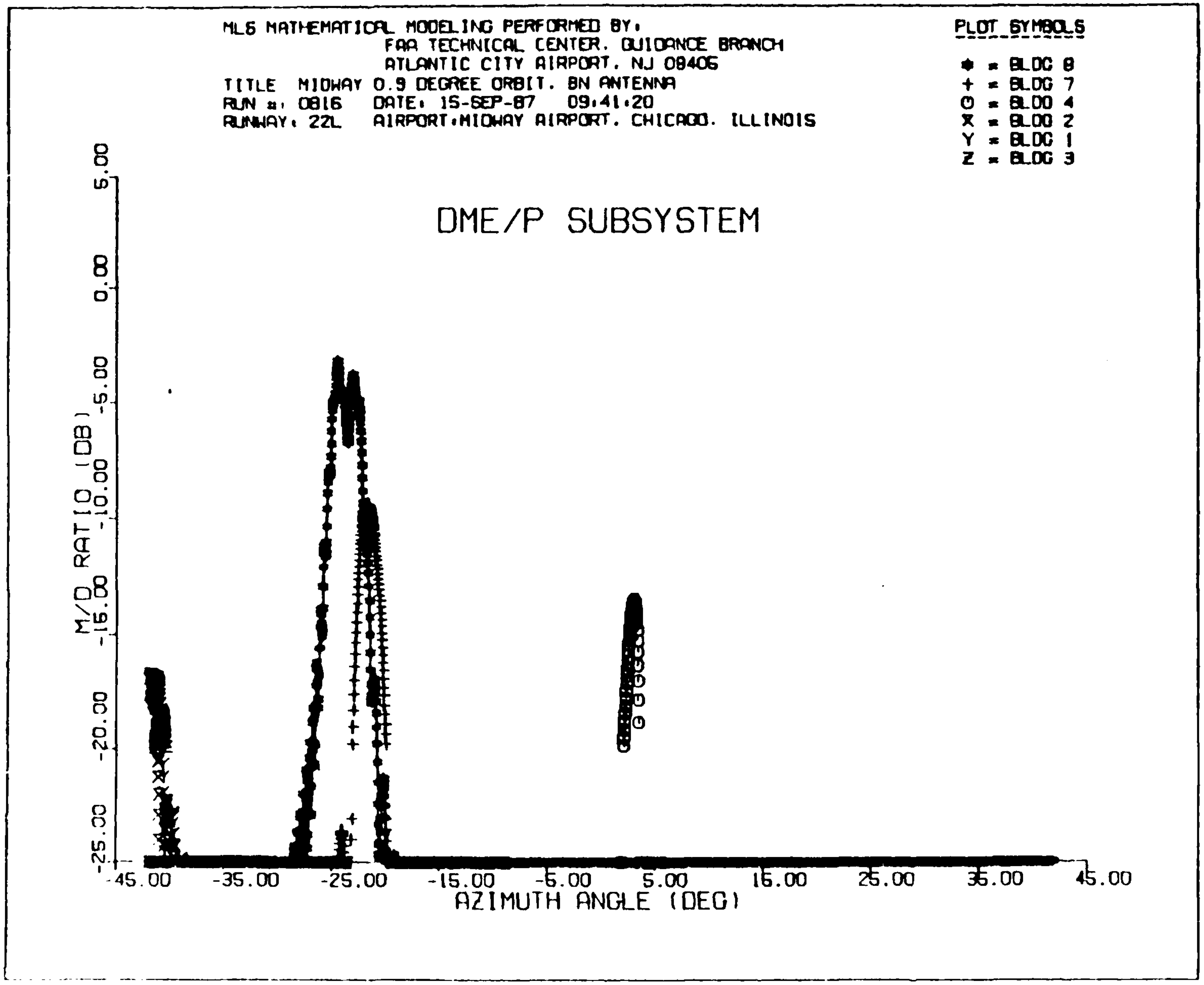

FIGURE 19 - MIDWAY RUNWAY 22L, ORBITAL FLIGHTPATH, DME/P SUBSYSTEM, MULTIPATH/DIRECT SIGNAL RATIO PLOT.

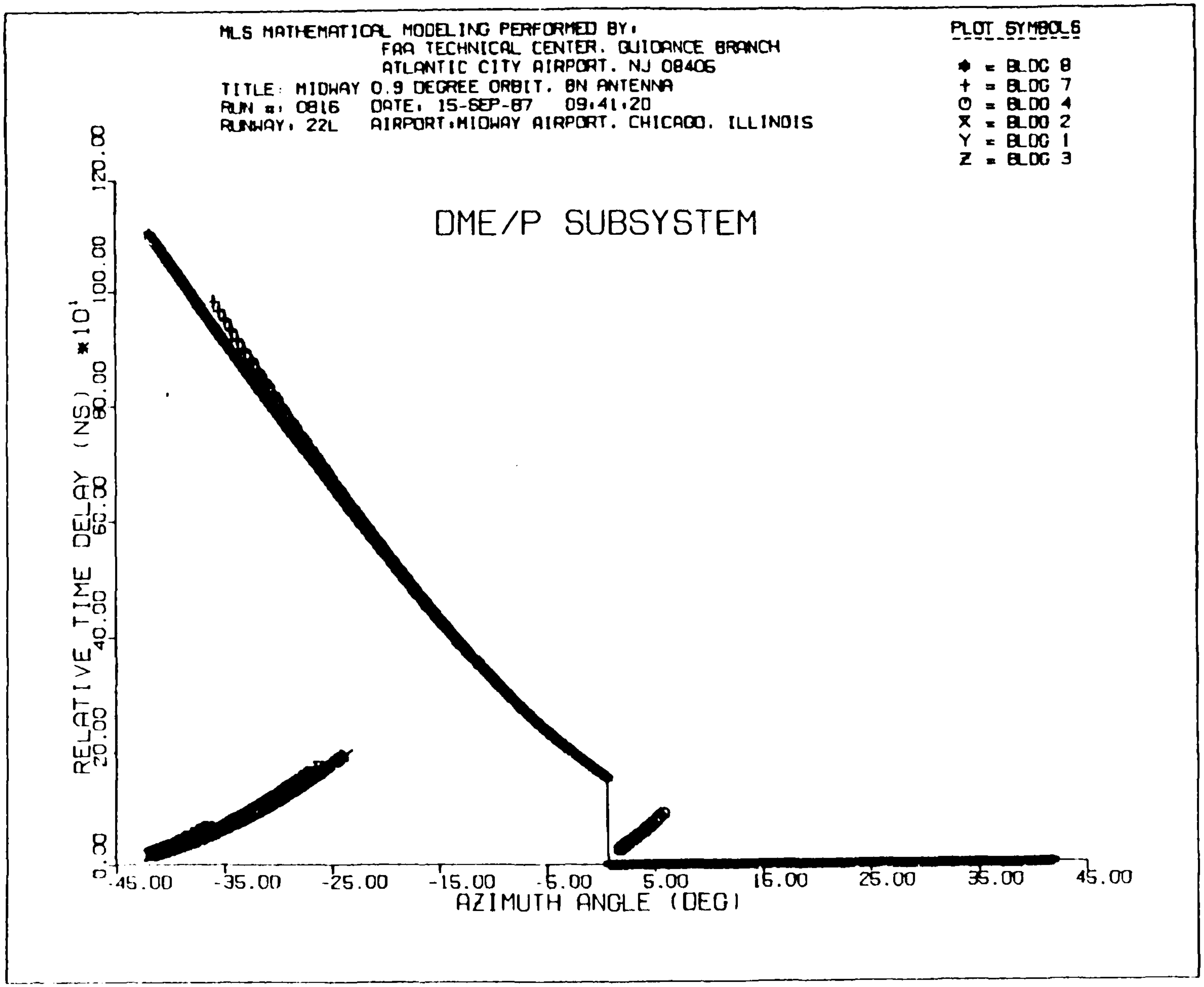

FIGURE 20 -- MIDWAY RUNWAY 22L, ORBITAL FLIGHTPATH, DME/P SUBSYSTEM, RELATIVE TIME DELAY PLOT.

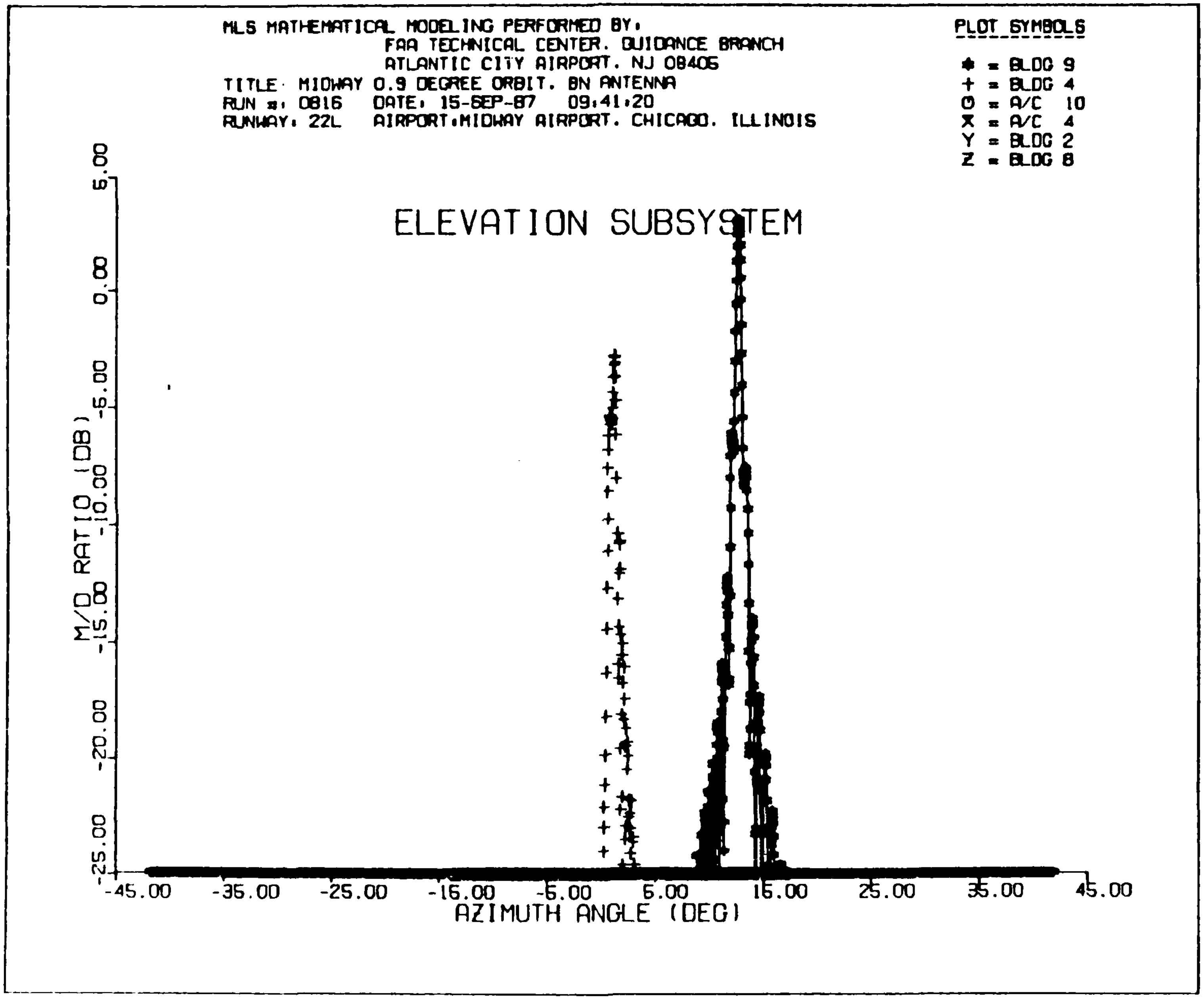

FIGURE 21 – MIDWAY RUNWAY 22L, ORBITAL FLIGHTPATH, ELEVATION SUBSYSTEM, MULTIPATH/DIRECT SIGNAL RATIO PLOT.

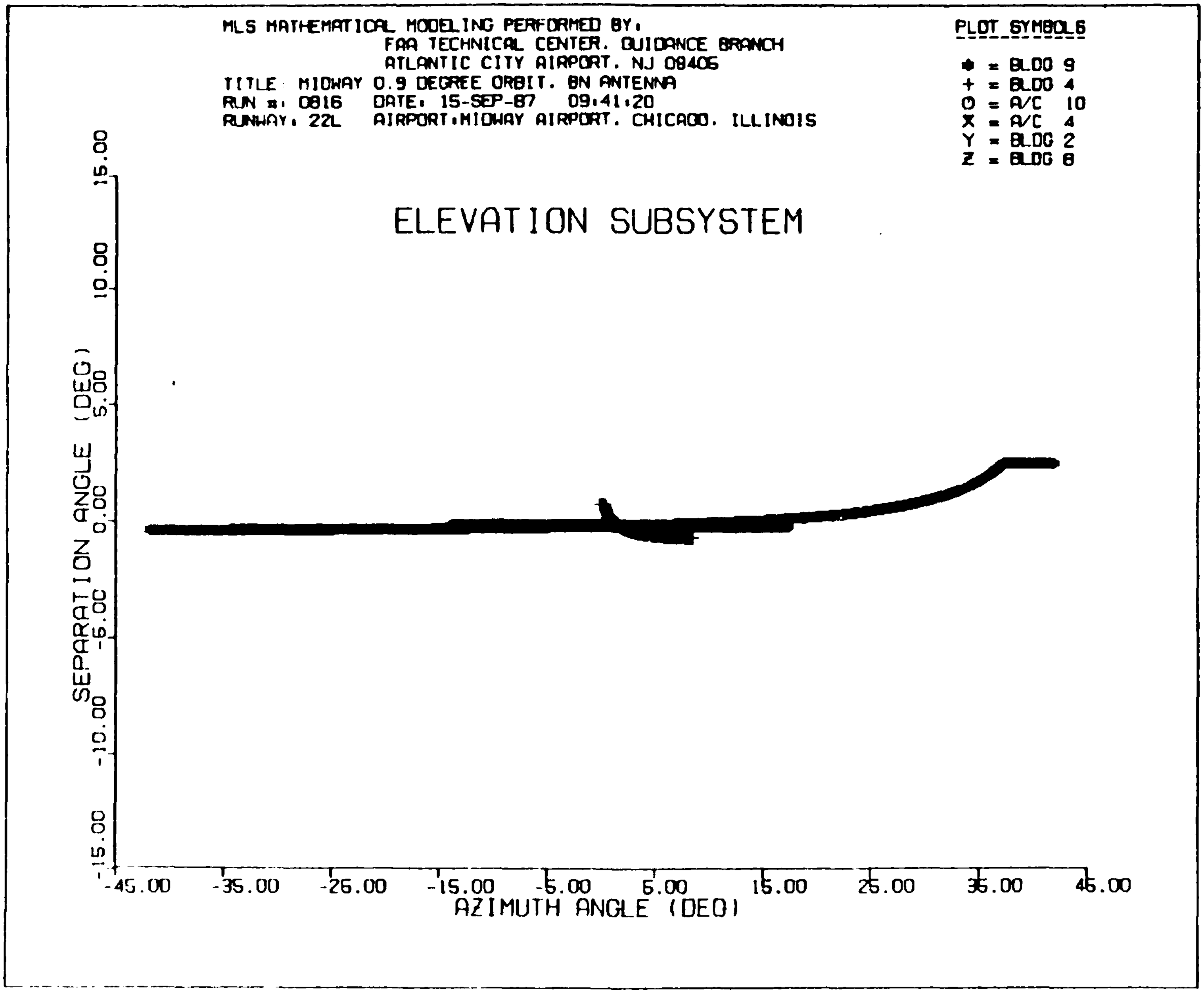

FIGURE 22 - MIDWAY RUNWAY 22L, ORBITAL FLIGHTPATH, ELEVATION SUBSYSTEM, SEPARATION ANGLE PLOT.

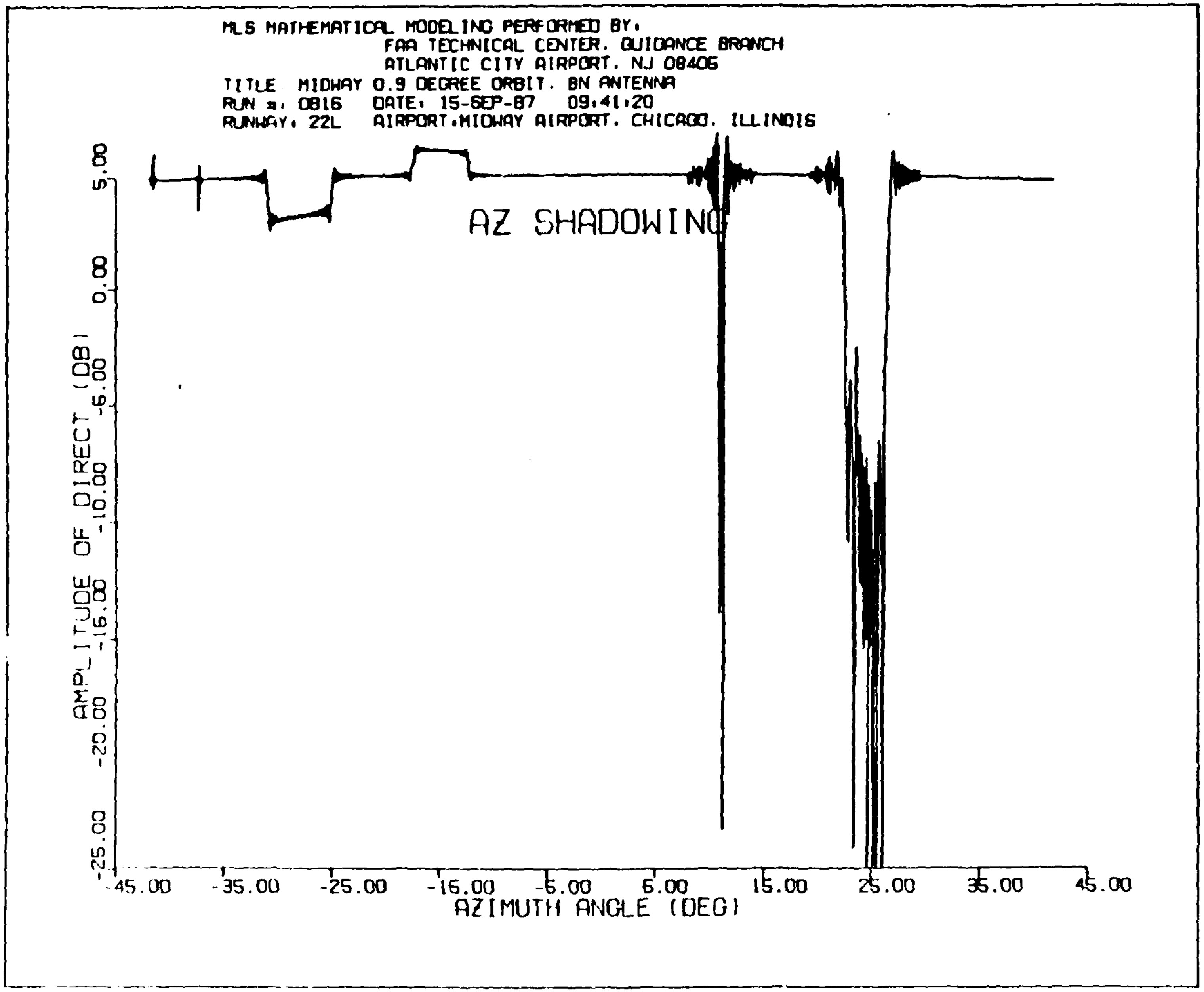

FIGURE 23 -- MIDWAY RUNWAY 22L, ORBITAL FLIGHTPATH, AZIMUTH SUBSYSTEM, SHADOWING PLOT.

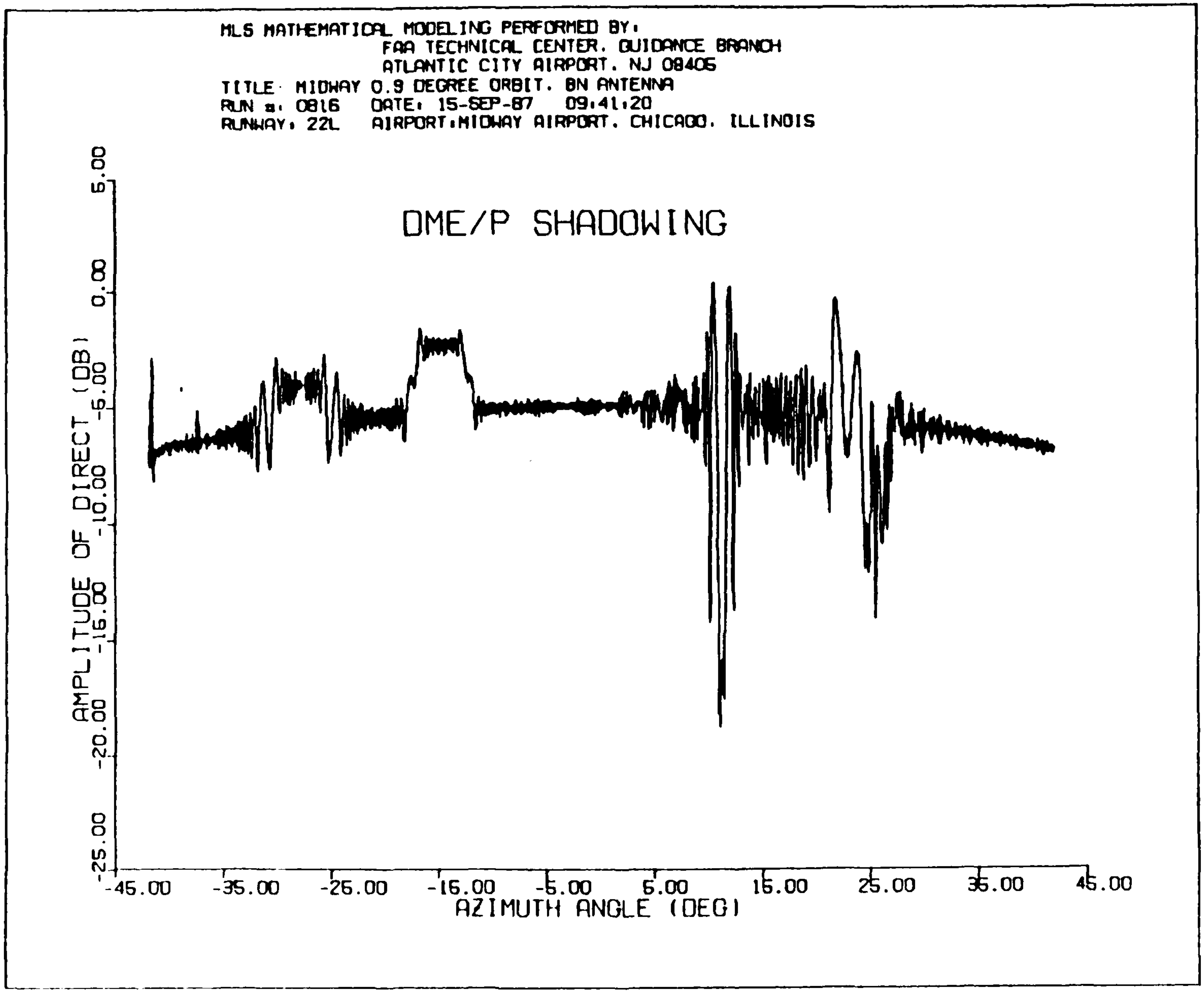

FIGURE 24 - MIDWAY RUNWAY 22L, ORBITAL FLIGHTPATH, DME/P SUBSYSTEM, SHADOWING PLOT.

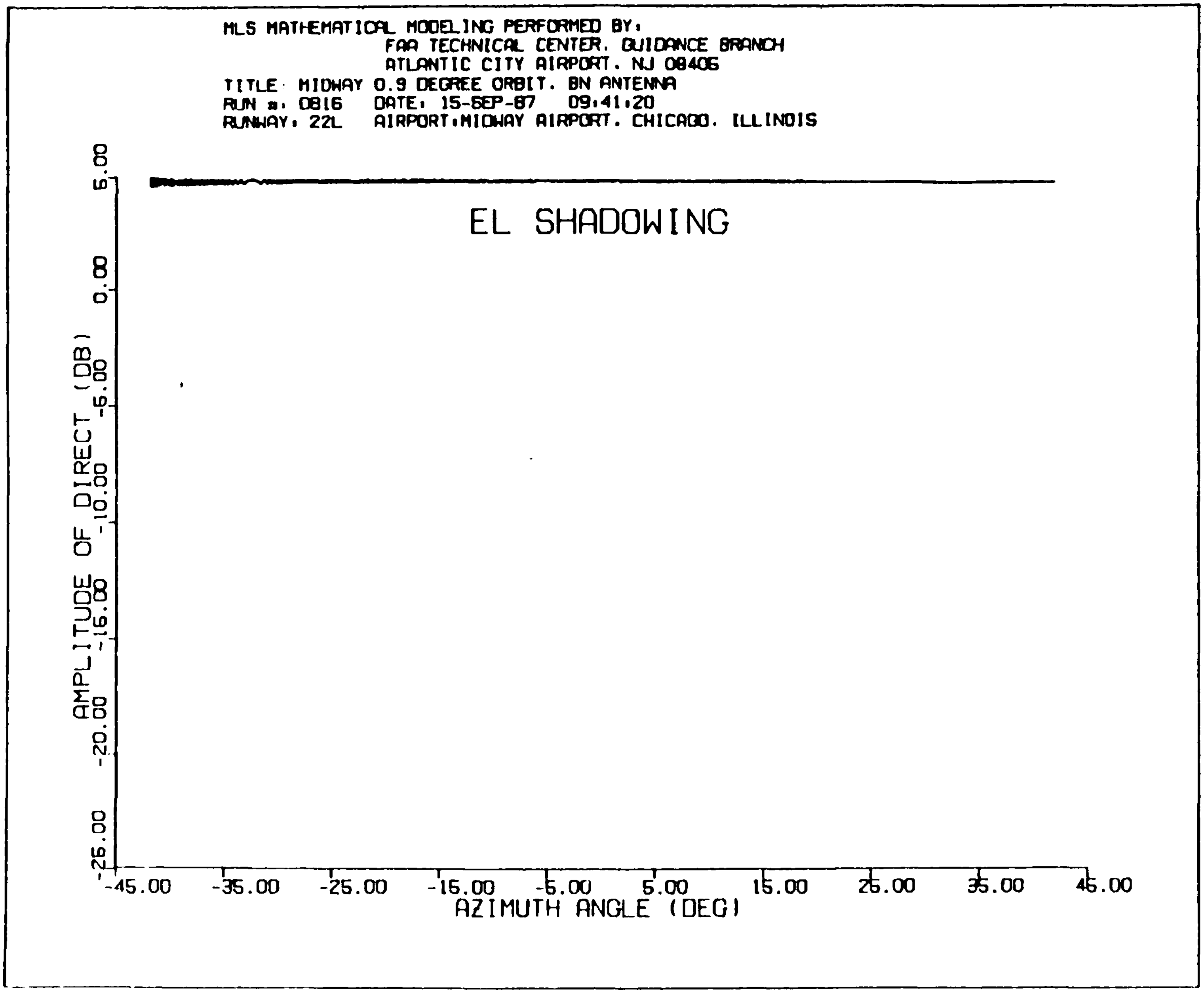

FIGURE 25 - MIDWAY RUNWAY 22L, ORBITAL FLIGHTPATH, ELEVATION SUBSYSTEM, SHADOWING PLOT.

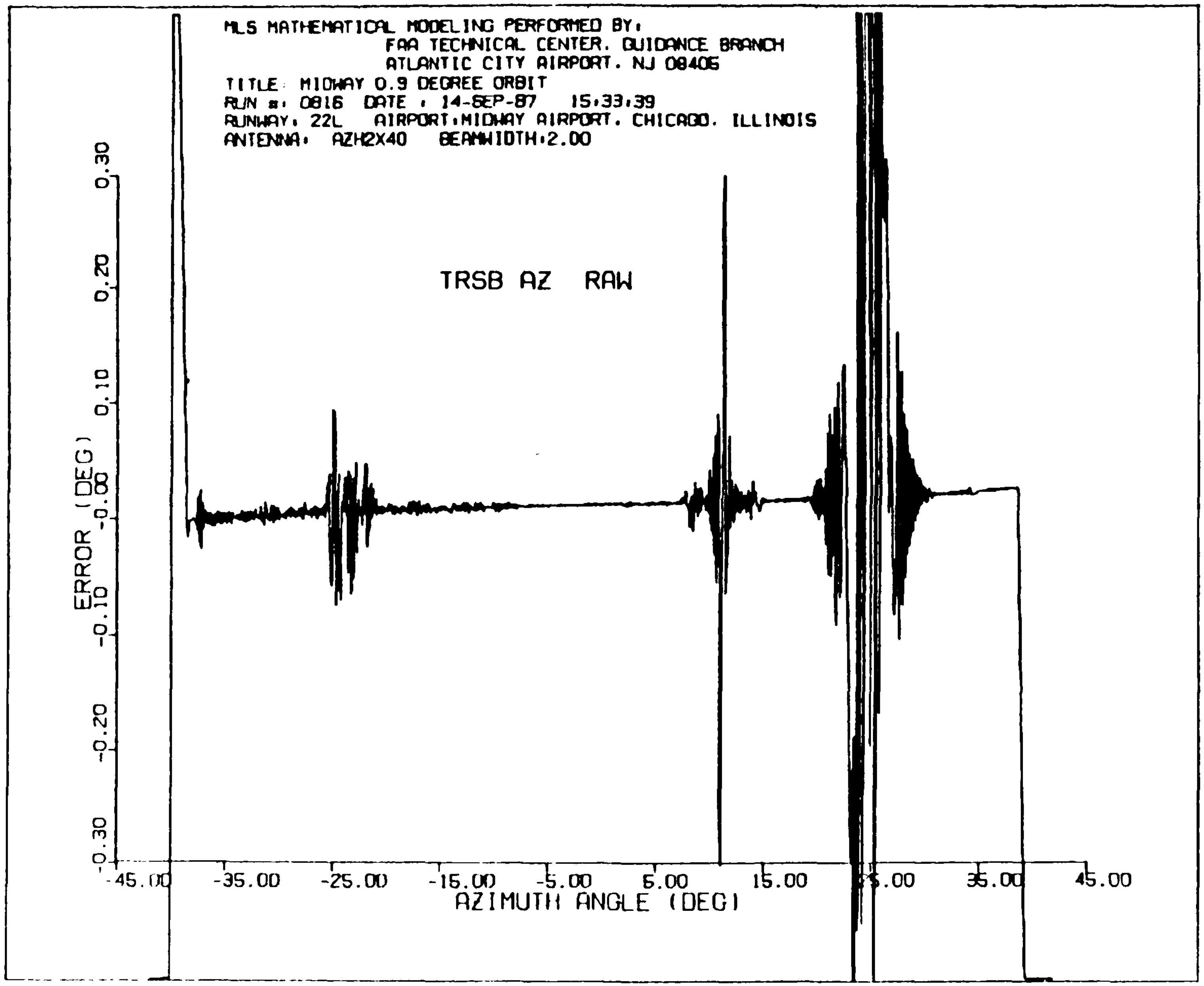

FIGURE 26 - MIDWAY RUNWAY 22L, ORBITAL FLIGHTPATH, AZIMUTH SUBSYSTEM, RAW ERROR PLOT.

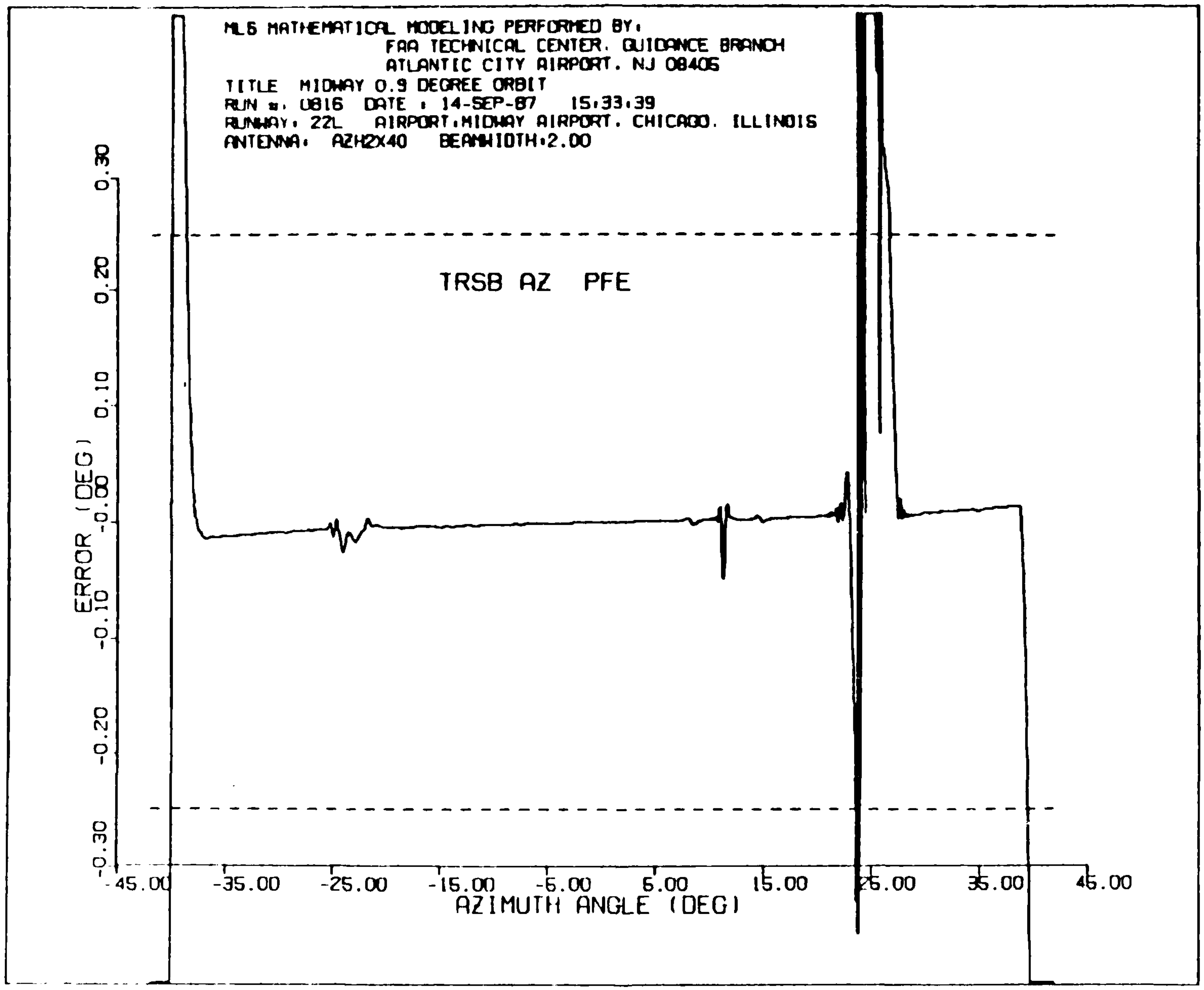

FIGURE 27 - MIDWAY RUNWAY 22L, ORBITAL FLIGHTPATH, AZIMUTH SUBSYSTEM, PFE FILTERED PLOT.

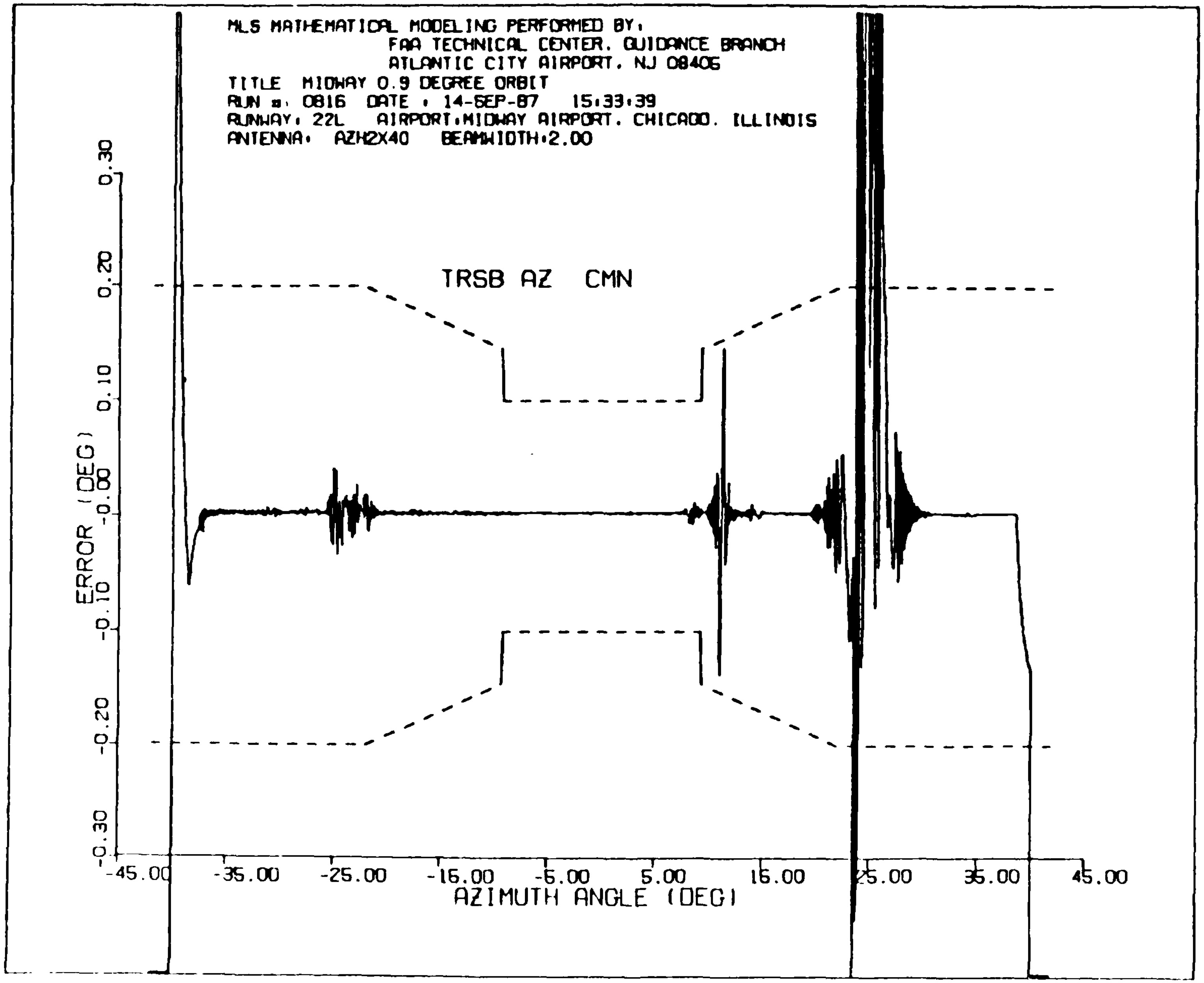

FIGURE 28 - MIDWAY RUNWAY 22L, ORBITAL FLIGHTPATH, AZIMUTH SUBSYSTEM, CMN FILTERED PLOT.

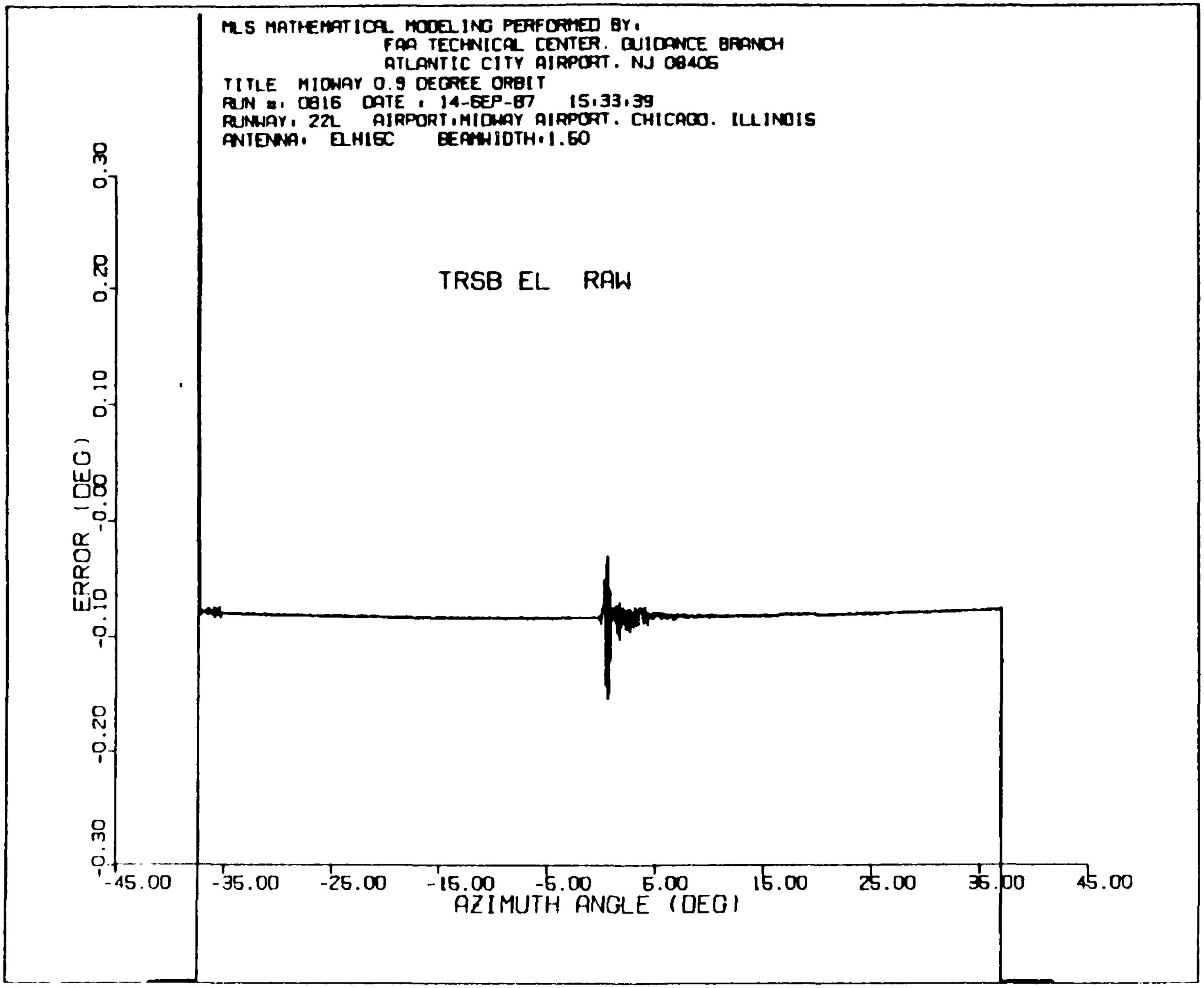

FIGURE 29 - MIDWAY RUNWAY 22L, ORBITAL FLIGHTPATH, ELEVATION SUBSYSTEM, RAW ERROR PLOT.

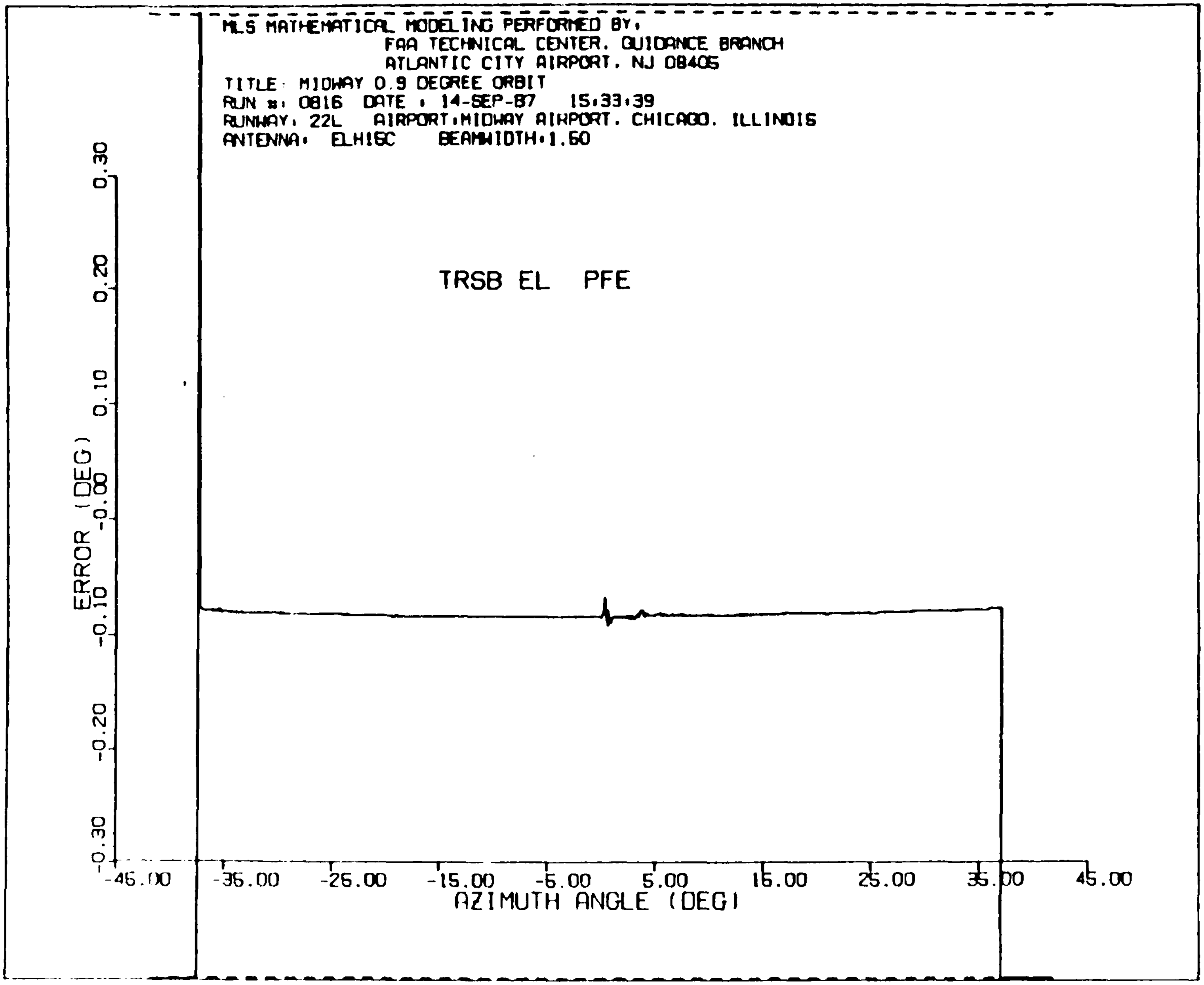

FIGURE 50 - MIDWAY RUNWAY 22L, ORBITAL FLIGHTPATH, ELEVATION SUBSYSTEM, PFE FILTERED PLOT.

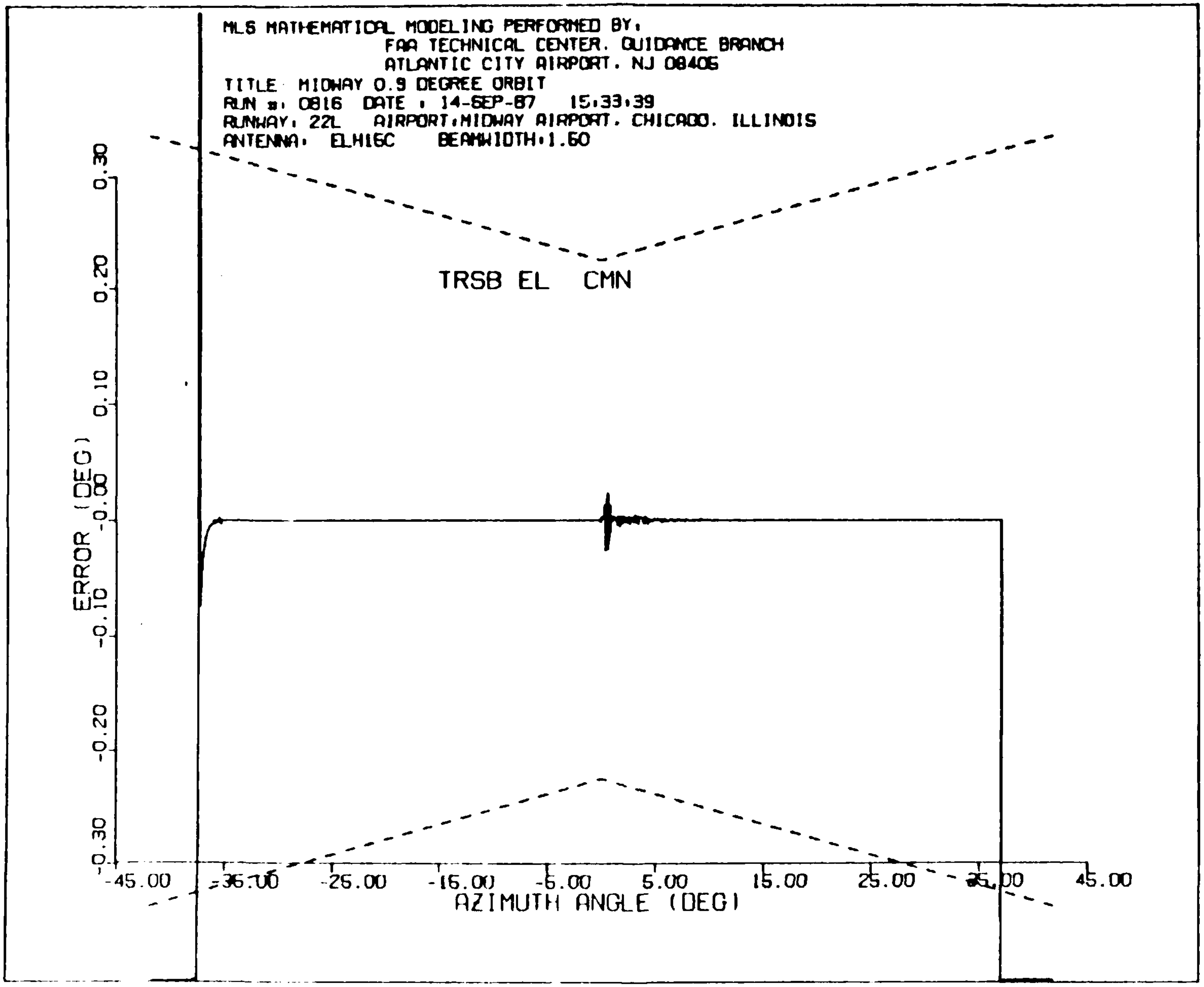

FIGURE 31 - MIDWAY RUNWAY 22L, ORBITAL FLIGHTPATH, ELEVATION SUBSYSTEM,
CMN FILTERED PLOT.

APPENDIX A

MICROWAVE LANDING SYSTEM (MLS) MATHEMATICAL MODEL DESCRIPTION

The MLS mathematical model simulation program is written in the FORTRAN 77 (ANSI X3.9-1978) computer language and has successfully been used on computers in the United States, United Kingdom, and the Federal Republic of Germany. An MLS simulation may be considered as consisting of three processes.

1. The first process is the creation of a formatted input file which defines the airport environment. This input data specifies the locations and composition of reflecting and shadowing obstacles, terrain features, antenna locations, and the simulated flightpath.

2. The second process is known as the propagation model. This program determines the signals at the receiver for each point along the flightpath, taking into account the various multipath reflections. The diagnostic plots obtained from the propagation model show which obstacles could cause significant multipath effects.

3. The third process is the Time Reference Scanning Beam (TRSB) system and receiver model. This part of the simulation computes the receiver error caused by multipath for the specified ground equipment antenna patterns, aircraft antenna pattern, scan format, and receiver processing algorithm. The raw errors computed by the system model are passed through PFE and CMN filter algorithms and plotted along with the applicable tolerance limits.

Figure A-1 shows the interrelationship of these processes to the total MLS simulation. (See Bibliography in text for detailed theory and description.)

AIRPORT/FLIGHTPATH MODEL.

The formatted input file consists of data specified for the particular airport environment being considered. At the Federal Aviation Administration (FAA) Technical Center, this information is currently entered in an interactive session which edits a standard input file template to add the appropriate data for input to the propagation model. The degree of approximation to an actual airport environment will depend heavily upon the simulation and the scatterer geometry. For example, in a case where the multipath is out of beam and of short duration, hangars might be represented by a single plate; however, to closely predict actual system performance in a critical multipath situation, it would be necessary to input the same hangar with many plates representing the various electrical properties of the different parts of the hangar.

PROPAGATION MODEL.

Propagation modeling consists of executing the propagation program with the formatted input file as input data. This model determines the multipath characteristics of the specified airport environment. The numerical results from the propagation model define the direct signal; signals reflected from or diffracted by terrain, buildings, and aircraft; and the changes in the direct

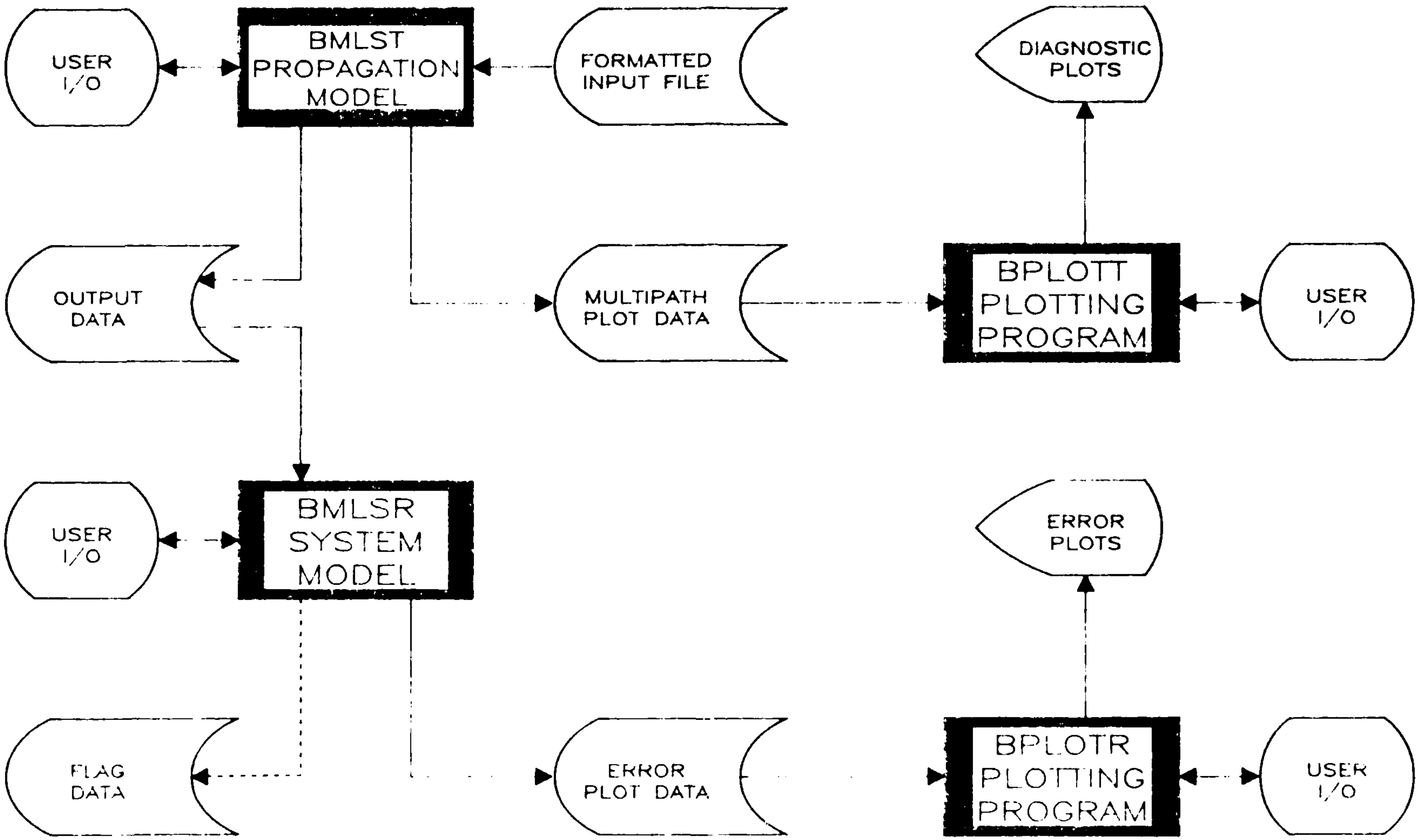

FIGURE A-1. MLS MATHEMATICAL MODEL DATA FLOW DIAGRAM signal characteristics due to shadowing by runway humps, buildings, and aircraft. The type of multipath considered in a simulation is dependent upon and determined by the input parameters specified. Numerical results are saved in two different files: one file for further processing by the system model (data set 8), and the other for plotting of the multipath data (data set 16). The propagation model can accommodate the multipath types specified below.

1. Terrain reflection modeling. The terrain is typically represented by a collection of rectangular and triangular plates, each with prescribed orientation, roughness, and dielectric constant. By varying these parameters, one can assess the sensitivity of performance to terrain type (e.g., dry ground versus snow). The multipath levels are computed either by a numerical Kirchoff-Fresnel integral or a simplified approximation.

2. Building reflection modeling. Buildings are represented by one or more rectangular plates of prescribed orientation and surface material. The various plates represent salient features of a building such as the doors of a hangar. By allowing each plate to have a different surface material characterization, inhomogeneous surfaces (e.g., concrete walls with metal doors) can be modeled. Consideration is also made for secondary ground reflection paths. The levels are computed assuming Fresnel diffraction and using closed form Fresnel integral expressions.

3. Aircraft reflection modeling. For aircraft, it is essential to consider the curvature of the surfaces as this tends to spread the reflections over a much greater region than would be the case with flat plates. The fuselages and tail fins are both modeled as cylinders or a section thereof. The resulting multipath levels are computed by a combination of Fresnel diffraction (integrals) and geometric optics.

4. Shadowing. Shadowing by buildings or aircraft causes both an attenuation and distortion of the transmitted wavefront. Both of these factors are considered in the models for shadowing. The shadowing obstacles are represented by one or more rectangular plates which approximate the object silhouette. Similar techniques have been successfully used in studying the effects of widebody aircraft on the Instrument Landing System (ILS). The shadowing of the azimuth signal by runway humps requires explicit consideration of the surface curvature and is computed by mathematical algorithms similar to those of aircraft reflection modeling.

PROPAGATION MODEL DIAGNOSTIC PLOTS. Graphical interface subroutines have been developed to display the model output on several alternate graphical display devices. The graphical routines generally used to display the propagation model results at the FAA Technical Center are from the TEKTRONIX Plot 10 Terminal Control System and CALCOMP Preview software. These routines provide easy access to the graphic capabilities of the Tektronix 4010 type Direct View Storage Tube (DVST) terminals. Information displayed on the storage tube may be copied as desired (via a hard copy unit) to provide a permanent record of the results. Graphical output from the multipath model consists of a listing of the input parameters used in the simulation, the flightpath of the receiver, an airport map showing the location of the transmitters and obstacles, and multipath diagnostics. These diagnostics display relative azimuth (AZ), distance measuring equipment (DME), and elevation (EL) multipath/direct (M/D) amplitude ratios (for the maximum component of the several multipath components from a given obstacle) and separation angles (time delay for DME) along the flightpath for the obstacles generating significant multipath components, and the variation in the direct signal AZ, DME, or EL level where shadowing is involved.

SYSTEM MODEL.

The TRSB system and the MLS receiver algorithms are simulated in the system model. This model considers the received signal as a superposition of the received direct path signal and a number of replicas (multipath) of it, each having its own amplitude, delay, angle, and Doppler shift. The system model then determines the receiver error by taking into account the nature of the transmitted signals and the antenna patterns. The functional form of the beam waveform is determined from measured or theoretical patterns and is included in the model as a function subprogram. By superimposing the beam patterns corresponding to the various signal paths, the net received envelope is determined.

The remainder of the system model parallels the processing by the receiver microprocessor. A tracking gate (dwell gate or split gate can be simulated) is centered on the largest consistent envelope peak with the beam arrival angle derived by finding the times at which the leading and trailing edges of the received envelope cross a threshold. Various checks and tracking algorithms are applied to each measurement before it is presented as angle data. DME is not a part of the system model at this time.

SYSTEM/RECEIVER MODEL PLOTTING.

The output of the system model is generally displayed on a Tektronix DVST using the TEKTRONIX Plot 10 and CALCOMP Preview graphics subroutines. A specific transmitter (AZ or EL) is selected for plotting and the raw (and static if desired) errors generated by the model are plotted versus the distance along the flightpath. The raw errors may be processed with digital PFE and CMN filtering algorithms. The resultant errors may be plotted against the applicable tolerance limits. An analysis of the filtered error plots shows whether the system is suitable for commissioning.

APPENDIX B

DESCRIPTION OF INPUT PARAMETERS DISPLAYED IN TABLES 1 AND 2

PARAMETERS REQUIRED FOR MULTIPATH COMPUTATIONS.

The following parameters are required to specify the airport model which is employed in the multipath computation section of the program. A standard rectangular coordinate system is used, where the X,Y-plane is in the plane of the runway, the X-axis is coincident with the runway center line and the Z-axis passes through the stop end of the runway. All lengths, frequencies, and times are given in feet, hertz (Hz), and seconds, respectively.

*TRANSMITTER PARAMETERS (AZIMUTH, PRECISION DISTANCE MEASURING EQUIPMENT, AND ELEVATION).

1. Azimuth - (X,Y,Z), Elevation - (X,Y,Z), DME/P - (X,Y,Z): X,Y,Z - coordinates of location of transmitter.

2. (AZ, EL, DME/P) FREQUENCY: Frequency of transmitter.

*PARAMETERS USED IN COMPUTATION OF MULTIPATH REFLECTIONS.

*Rectangular Surface Elements are:

1. ID: Two-character surface identification.

2. (X1, Y1, Z1), (X2, Y2, Z2), (X3, Y3, Z3): X,Y,Z-coordinates of two corners, plus X,Z coordinates of third corner, in increasing order of magnitude for the X-coordinate, for each rectangular surface element.

3. ERSR, ERSI, SH2S: The real and imaginary relative dielectric constants, and the root-mean-square roughness height, respectively, for each rectangular surface element.

4. NRSPEC: Rectangular ground surface flag.

*Triangular Surface Elements are:

1. ID: Two-character surface identification.

2. (X1, Y1, Z1), (X2, Y2, Z2), (X3, Y3, Z3): X,Y,Z-coordinates of the three corners of each triangular surface element, in increasing order of magnitude of the X-coordinate.

3. ERSR, ERSI, SH2S: The real and imaginary relative dielectric constants, the root-mean-square roughness height, respectively, for each triangular surface element.

4. NTSPEC: Triangular ground surface flag.

*Default Values for Surface Elemenys and Ground are:

1. ISPGRD: Focusing ground computation flag.

2. ERO, SH2O: Default values of dielectric constant and roughness height which are used in those regions not specified by previously defined rectangular and triangular areas.

3. ERG, SH2G: Dielectric constant and RMS roughness height for ground reflection. These parameters are specified only once, since they are assumed to be the same for the ground surrounding all buildings and aircraft.

*Building Parameters are:

1. ID: two-character building identification.

2. (XL, YL), (XR, YR): X, Y-coordinates of left-hand and right-hand edge of face of each building.

3. HB: Height of building, relative to bottom edge, for each building.

4. HBOT: Height of bottom edge above Z-axis reference plane.

5. SH2B, ERBR, ERBI: The RMS roughness height and real and imaginary relative dielectric constants.

6. BTILT: Tilt angle of building. This angle is positive if building has positive Y coordinates and tilts away from the centerline r if building has negative Y coordinates and tilts towards the centerline. Otherwise this angle is negative.

7. GRNDBD: Differential height factor of ground on paths to and from the hangar, i.e., height of ground beside the runway relative to the runway height. This factor is positive if ground is above zero height level and negative otherwise.

The parameters ERG and SH2G specified in item 3 under "Default Values for Surface Elements and Ground" are also used to obtain scattering from the building surfaces.

*Aircraft Parameters are:

1. ID: two-character aircraft identification.

2. (XT, YT), (XC, YC): X, Y-coordinates of cockpit and tail fin ends of fuselage centerline of each aircraft.

3. NACTYP: Aircraft type, for each aircraft, e.s.:

1 = 747
2 = 707-320B
3 = 727
4 = DC10
5 = C-124
6 = Convair 880
7 = Hastings aircraft
8 = Water tower
9 = Small diameter pipe
11 = C-5A
12 = C-141

A subroutine ACTYPE is called, using the appropriate aircraft type, to load the following aircraft parameters, which are already stored in computer memory, into a suitable storage area:

1. Area of wings
2. Radius of fuselage
3. Length of fuselage
4. Radius of curvature of tail fin
5. Width of tail fin
6. Height of tail fin
7. Height of center of fuselage above ground

4. ALT: Altitude of each aircraft defined as the height of fuselage centerline above the ground (Z-axis reference plane). If aircraft is parked on the ground, ALT should be set to zero so the program can recognize that a default value should be used in computations.

5. GRNDAC: Differential height factor of ground, i.e., height above zero of ground near side of runway.

The parameters ERG and SH2G specified in item 3 under "Default Values for Surface Elements and Ground" are also used to obtain ground reflections for scattering from the fuselage and tail fin.

*PARAMETERS USED IN COMPUTATION OF SHADOWING.

*Building Parameters are:

1. ID: Two-character building identification.

2. (XL, YL), (XR, YR): X,Y-coordinates of left-hand and right-hand edge of each shadowing surface.

3. HBS: Height of shadowing surface relative to bottom edge.

4. HBT: Height of bottom edge of surface relative to Z-axis reference plane.

*Runway Hump Shadowing Parameters are:

HUMPF, HUMPM, HUMPB: X,Y,Z-coordinates for the location of the hump along the runway.

The runway hump is assumed to extend from the lower to the upper edge of the runway. The peak of the runway coincides with HUMPB but does not pass through HUMPF and HUMPB unless they are symmetrical about HUMPM.

*Aircraft Parameters are:

1. ID: Two-character aircraft identification.

2. SHPOS1: X, Y, Z-coordinates of center of fuselage of each shadowing aircraft at the starting frame number.

3. SHPOS2: X, Y, Z-coordinates of center of fuselage of each shadowing aircraft at the ending frame number (assumes linearpath).

4. SHACTYP: Aircraft type (see item 3 under "Aircraft Parameters" above).

5. SHVEL: Velocity of shadowing aircraft between SHPOS1 and SHPOS2.

6. SHANG: Pitch angle, angle between fuselage centerline and the X-axis measured in the X-Z plane.

APPENDIX C

DESCRIPTION OF PATH FOLLOWING ERROR (PFE) AND CONTROL MOTION NOISE (CMN) FILTER EQUATIONS

The math model output data are processed through standard filters in order to assess the effects of the time reference scanning beam (TRSB) errors on actual aircraft movements and on control surface and stick motion.

PFE is defined as the theoretical worst case deviations from a preselected course of an aircraft following microwave landing system (MLS) guidance commands. CMN is that portion of the error which affects control surface, wheel, column motion, and aircraft attitude. Rate noise is a measure of the rate error in a bandpass region which would affect aircraft guidance accuracy.

PFE's, CMN, and rate errors are determined by passing the time records through standardized filters, described herein. The filter characteristics are based on a wide range of existing aircraft response properties and are believed to be adequate for any foreseeable aircraft as well.

Only PFE's and CMN errors are currently used in the analysis of math model output.

TABLE C-1. CRITICAL FREQUENCIES

Function	Critical Frequencies (RAD/sec [illegible])					
	W_c	W_n	W_1	W_2	$W_{[illegible]}$	$W_{[illegible]}$
AZ	0.5/0.08	0.78/0.12	0.3/0.05	10.0/1.59	[illegible]	[illegible]
EL	1.5/0.24	2.34/0.37	0.5/0.08	10.0/1.59	[illegible]	[illegible]
DME	2.0/0.32	3.13/0.50	0.5/0.08	10.0/1.59	[illegible]	[illegible]

PFE.

The actual aircraft perturbations caused by MLS errors are a function of the guidance loop bandwidth. The aircraft perturbations or PFE will be estimated using a path following filter. The transfer function of this filter is as follows:

$$H(s) = \frac{W_n^2}{(s^2 + 2\delta W_n s + W_n^2)}$$

$$W_o = 0.64 W_n \text{ for } \delta = 1$$

After applying a bilinear transform to this function we obtain the following digital filter difference equation which is implemented in the model:

$$Y_n = \frac{1}{(4 + 4\delta W_n T + W_n^2 T^2)} *$$

$$[W_n^2 T^2 (X_n + 2X_{n-1} + X_{n-2}) + (8 - 2W_n^2 T^2) Y_{n-1} - (4 - 4\delta W_n T + W_n^2 T^2) Y_{n-2}$$

CMN.

CMN is noise which causes control surface motion, column motion, and wheel motion, but does not significantly affect aircraft position. The CMN's will be estimated using a control motion filter. The transfer function of this filter is as follows:

$$H(s) = \frac{s}{s + W_1} * \frac{W_2}{s + W_2}$$

After applying a bilinear transform to this function we obtain the following digital filter difference equation which is implemented in the model:

$$Y_n = \frac{1}{(2 + W_1 T)(2 + W_2 T)} *$$

$$[2W_2 T (X_n - X_{n-1}) + (8 - 2W_1 W_2 T^2) Y_{n-1} - (W_1 T - 2)(W_2 T - 2) Y_{n-2}]$$

where :

X_n = Input at time n
Y_n = Output at time n
T = Sampling period
W_n = Critical frequency

APPENDIX D

COMPUTATION OF MLS SYSTEM COORDINATES

Midway runway 22L

General information required: Enter appropriate values.

Runway Length (ft) =	Lr := 5346	=6102-756
Runway Width (ft) =	Wr := 150	
Threshold Crossing Height (ft) =	ARDH := 55	
Glide Slope Approach Angle (deg) =	MGPA := 3.6	
Final Approach Fix (FAF) (nm) =	FAF := 6.241587	
MSL reference value (ft MSL) =	Zref := 605	
Threshold MSL (ft) =	Zth := 605	
StopEnd MSL (ft) =	Zse := 619	

Initializations:

$$deg := \frac{\pi}{180}$$

$$Ztch := Zth + ARDH$$

$$MGPA := MGPA \cdot deg$$

Runway Profile: Enter X and Z values along centerline.

$$nrpp := 7$$

$$i := 0 \,..(nrpp - 1)$$

$XR_i :=$	$ZR_i :=$
0	619
550	619
1375	613
2950	610
3750	608
5325	606
6102	605

Terrain Profile: Enter Y value of EL offset as well as X and Z values along the offset.

$Y_{el} := 325$

$nop := 15$

$j := 0 ..(nop - 1)$

$XE_j :=$	$ZE_j :=$
4050	606.8
4150	607.0
4250	606.7
4350	606.3
4450	606.0
4550	606.0
4650	605.8
4750	605
4850	606
4950	605
5050	604.9
5150	605.2
5250	605.4
5350	605.1
5450	605.2

EL phase center is 8 feet above ground. Therefore

$ZEPC_j := ZE_j + 8$

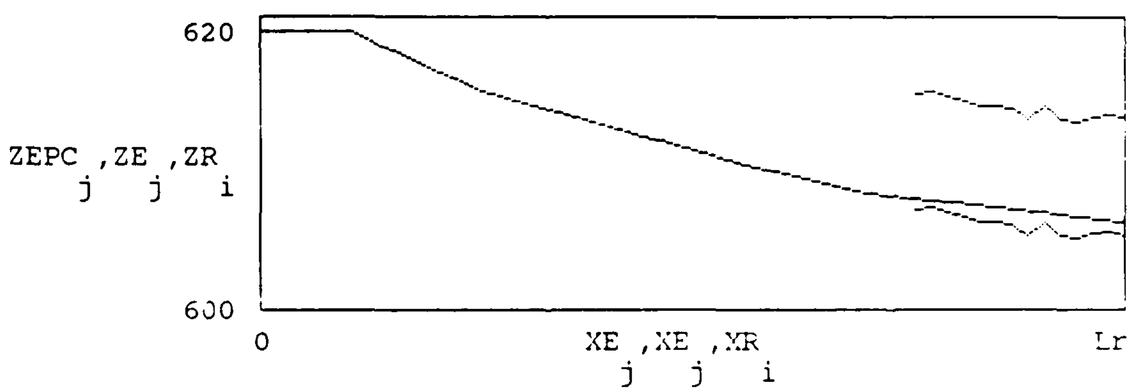

Equation of EL phase center constrained by known values at threshold.
X value is variable.

$E := lspline(XE, ZEPC)$

$Zepc(X) := interp(E, XE, ZEPC, X)$

$Zc(X) := Zepc(X) + \tan(MGPA) \cdot (Lr - X)$

$X := \min(XE)$

$Xel := root((Ztch - Zc(X)), X) \qquad X_{el} := Xel$

$Z_{el} := Zepc(Xel) - Zref$

****
ELEVATION COORDINATES

$X_{el} = 4614.725752$

$Y_{el} = 325$

$Z_{el} = 8.992095$

****

$Zfp(X) := Z_{el} + \tan(MGPA) \cdot \left[X - X_{el}\right]$

$R := lspline(XR, ZR)$

$Zrs(X) := interp(R, XR, ZR, X) \qquad Zrs(1) = 619.001092$

$X_d := X_{el} \qquad Zrs(Lr) = 605.976471$

$Y_d := 0$

$Z_d := Zrs\left[X_{el}\right] - Zref$

****
DATUM COORDINATES

$X_d = 4614.725752$

$Y_d = 0$

$Z_d = 1.72063$

****

$X := 0$

$XFP_1 := FAF \cdot 6076.1 + Lr \qquad YFP_1 := 0$

$$ZFP_1 := Z_{el} + \tan(MGPA) \cdot \left[XFP_1 - X_{el}\right]$$

$XFP_2 := root((Zfp(X) - (Zrs(X) - Zref + 8)),X)$

$YFP_2 := 0$

$$ZFP_2 := Z_{el} + \tan(MGPA) \cdot \left[XFP_2 - X_{el}\right]$$

$i := 0 ..(nrpp - 1)$

$$npp := \sum_i \Phi\left[XFP_2 - XR_i\right]$$

$i := npp, (npp - 1) ..1$

$XFP_{3+npp-i} := XR_{i-1}$

$i := 3 ..npp + 2$

$YFP_i := 0$

$i := npp, (npp - 1) ..1$

$ZFP_{3+npp-i} := ZR_{i-1} + 8 - Zref$

****

FLIGHTPATH PROFILE

$i := 1 ..npp + 2$

XFP_i	YFP_i	ZFP_i
43270.506771	0	2441.007695
4626.110237	0	9.708346
3750	0	11
2950	0	13
1375	0	18
550	0	22
0	0	22

END
DATE
FILMED
5-88
DTIC